6/p

NACA

RESEARCH MEMORANDUM

EFFECTS OF SOME CONFIGURATION CHANGES ON AFTERBURNER COMBUSTION PERFORMANCE

By Shigeo Nakanishi and Charles R. King

Lewis Flight Propulsion Laboratory
Cleveland, Ohio

NATIONAL ADVISORY COMMITTEE
FOR AERONAUTICS

WASHINGTON

June 12, 1957

[redacted]

NACA RM E57C01

NATIONAL ADVISORY COMMITTEE FOR AERONAUTICS

RESEARCH MEMORANDUM

EFFECTS OF SOME CONFIGURATION CHANGES ON AFTERBURNER COMBUSTION PERFORMANCE

By Shigeo Nakanishi and Charles R. King

SUMMARY

An experimental investigation was conducted in a 25.75-inch-diameter simulated-afterburner test rig at the NACA Lewis laboratory to determine the effects of some configuration variations on afterburner combustion performance. The variations included a V-gutter flameholder with the maximum gutter-ring diameter reduced from 20 (reference configuration) to 17 inches, but with equal projected blockage; an inclined radial-gutter flameholder; a tapered-shell afterburner; and a V-gutter flameholder with turbulence generators added.

The investigation was conducted over a range of afterburner fuel-air ratios from lean blowout to about 0.08; afterburner-inlet pressures from 750 to 1800 pounds per square foot absolute; afterburner-inlet gas temperatures from 1260° to 1660° R; afterburner-inlet velocities from about 350 to 650 feet per second; and, in some configurations, afterburner lengths from $3\frac{1}{2}$ to $5\frac{1}{2}$ feet. The combustion efficiency, lean blowout limits, and afterburner pressure-loss coefficient of each configuration were compared at matched inlet flow conditions with a conventional high-performance V-gutter configuration taken as a reference.

The reduction in V-gutter flameholder diameter caused a considerable loss in efficiency at flow conditions and afterburner lengths generally unfavorable for efficient combustion. At favorable conditions, the loss in efficiency was small. The lean limits at high velocities were slightly better, and the pressure-loss coefficient at high afterburner temperature ratios was somewhat greater, than those for the reference configuration. The inclined radial-gutter flameholder gave equal or slightly poorer combustion efficiency, better lean blowout limits, and higher pressure-loss coefficient than the reference configuration.

The efficiency of the tapered-shell afterburner compared with that of the reference cylindrical afterburner having an equivalent combustion-chamber volume was approximately the same at an afterburner-inlet velocity of 400 feet per second, but degenerated more rapidly with increasing

afterburner-inlet velocity. Lean blowout limits also narrowed more rapidly as the afterburner-inlet velocity increased. The pressure-loss coefficient during afterburning operation was higher in the tapered afterburner but practically identical with the cylindrical afterburner during nonafterburning operation.

The addition of turbulence generators 12 inches downstream of the gutter trailing edge of the V-gutter flameholder resulted in lower efficiency, poorer lean blowout limits, and considerably higher pressure-loss coefficient than those of the reference configuration, especially at the higher afterburner-inlet velocities.

INTRODUCTION

The ever-widening spectrum of high-speed flight imposes new and greater demands upon turbojet-aircraft propulsion systems. One of the propulsion-system components affected is the afterburner. In designs where the use of an afterburner is considered, the specifications become quite rigid, not only in terms of performance required at severe operating conditions, but also in terms of geometrical changes often made necessary by space and structural limitations.

Afterburner combustion performance is influenced by many individual factors and their mutual interaction. Fuel properties and reaction kinetics are some of the factors which are chemical in nature. Pressure, temperature, and velocity of the mixture approaching the afterburner combustion chamber are aerothermodynamic factors. Still other factors such as flameholder gutter dimensions and gutter arrangement are of a geometrical nature. These and other factors both singly and collectively affect the performance of a given afterburner. For example, the flame spreading rate, which controls combustion efficiency, depends upon both aerothermodynamic and chemical factors.

Combustion principles applicable to afterburners, together with results of some previous NACA research programs, are summarized in references 1 to 3. The effects of inlet flow variables and afterburner combustion-chamber length on combustion performance are reported in reference 4.

As a sequel to the investigation of reference 4, an experimental investigation was conducted at the NACA Lewis laboratory to determine the effects of some configuration changes on afterburner performance. The purpose of this report is to present the final results of this investigation (some advance information of which is reported in ref. 3) in its entirety.

The configurations investigated were (1) a reduced-diameter V-gutter flameholder, (2) an inclined radial-gutter flameholder, (3) an afterburner with a tapered shell, and (4) a V-gutter flameholder with turbulence generators added. The tests with the reduced-diameter flameholder were made in order to evaluate the changes in afterburner performance associated with a variation in flameholder gutter-ring diameter while holding the projected blockage constant. Some results of comparable variations made in a two-dimensional duct are reported in reference 5. In practical afterburner applications, reduction of the flameholder gutter diameter may be necessary to alleviate a serious afterburner-shell cooling problem.

The inclined radial-gutter flameholder was designed to combine the simplicity and low-pressure-loss characteristics of the annular gutter-type flameholder with the inherent stability and high efficiency of the can-type combustor. Such a flameholder, initially designed and reported in reference 6, has been successfully used in a ram-jet combustor. The present investigation sought to determine the applicability to and the performance of this type of flameholder in an afterburner.

The tapered-shell afterburner was investigated in order to evaluate the penalties in performance caused by tapering the afterburner shell to conform to space or structural limitations. These limitations are particularly acute in pod-mounted installations and fuselages designed for minimum afterbody drag.

Turbulence generators were mounted downstream of the V-gutter flameholder in order to evaluate the effects of mechanically introducing turbulence in the fuel-air mixture approaching the flame fronts. Some investigators have found a direct relation between turbulence and rate of flame spreading. The present tests sought to determine whether such a relation would manifest an improvement in afterburner performance. Another investigation of this nature has been conducted over a limited range of operating conditions and is reported in reference 7.

The preceding configurations were investigated over a range of afterburner fuel-air ratios from lean blowout to about 0.08; afterburner-inlet pressures from 750 to 1800 pounds per square foot absolute; afterburner-inlet gas temperatures from 1260° to 1660° R; afterburner-inlet velocities from 350 to 650 feet per second; and, in some configurations, afterburner lengths from a minimum of $3\frac{1}{2}$ feet to a maximum of $5\frac{1}{2}$ feet.

Effects of each configuration change are shown by comparison with the performance of a conventional V-gutter configuration taken as a reference. The reference configuration is representative of good present-day design, and its performance is presented over a wide range of operating conditions in reference 4. All comparisons were made at operating conditions matched as closely as possible.

[redacted]

APPARATUS

Installation

A schematic layout of the simulated-afterburner test rig is shown in figure 1. Combustion air controlled at the inlet airflow valve was preheated by the direct combustion of fuel in eight turbojet combustors. The hot gases attained a uniform temperature in the mixing chamber. The air measuring screen ahead of the diffuser served to meter the gas flow and also to promote a circumferentially uniform flow distribution in the diffuser flow passage. Fuel introduced into the gas stream through fuel bars formed a combustible mixture which was ignited and stabilized on the flameholder. The variable-area nozzle at the exit of the afterburner permitted control of the afterburner-inlet velocity at any afterburner temperature ratio and pressure. Other details of the test rig and its operation as well as a description of the reference configuration may be found in reference 4. The basic inside diameter of the afterburner was 25.75 inches. Geometrical details and dimensions of the reference-configuration flameholder are shown in figure 2. The projected blocked area of this flameholder was 29.6 percent of the afterburner cross-sectional area.

Configuration Changes

Reduced-diameter flameholder. - A schematic sketch of the reduced-diameter flameholder is shown in figure 3. The maximum diameter of the outer gutter ring was 3 inches less than that of the reference configuration, thus increasing the distance between gutter edge and afterburner wall from 2.875 to 4.375 inches. The total projected blocked area, as well as the number of gutter rings and interconnecting gutters, was held constant. This resulted in gutter elements that were 0.5 inch wider than the reference elements. Constant-diameter afterburner shells of $3\frac{1}{2}$ and $5\frac{1}{2}$ feet in length were used in the investigation.

Inclined radial-gutter flameholder. - Two views of the inclined radial-gutter flameholder are shown in figure 4. The photograph of figure 4(a) shows the front view or the view looking downstream in the direction of the gas flow. The central V-gutter ring and the outer half-V-gutter ring (the straight side of which extends to form a cooling liner) are interconnected by radial gutters inclined in the direction of the flow.

A schematic diagram of the configuration with the flameholder installed is shown in figure 4(b). The long cooling-liner configuration constructed by welding a hollow cylindrical shell to the original cooling liner is indicated by dotted lines. The afterburner length for both the short- and long-liner configurations was $4\frac{1}{2}$ feet.

[redacted]

Tapered-shell afterburner. - A schematic drawing of the tapered afterburner is shown in figure 5. The basic cylindrical afterburner diameter was maintained 6 inches downstream of the trailing edge of the flameholder, followed by a degree of taper selected on the basis of the most rigid space requirements expected of a typical aircraft installation. The particular afterburner used in the present investigation had a 5° wall taper and 14.3 percent less afterburner volume than a cylindrical afterburner of the same length.

A series of fixed-area conical exit nozzles were used in place of the adjustable-area exhaust nozzle, which fits only the reference-configuration afterburner duct. Afterburner-inlet velocity was thus varied by changing the fixed-area nozzles.

Turbulence generators. - The two types of turbulence generators added to the reference-configuration flameholder are shown in figure 6. The turbulence generator of figure 6(a) owes its origin to the tip-vortex generators often used to improve subsonic-diffuser performance. The radial-vane mixer of figure 6(b) consists of thin vanes twisted and mounted to impart flow deflection and rotation. Mixers of this type have been used in the diffuser passage of some turbojet compressors to promote a more uniform velocity profile.

Schematic diagrams of the turbulence generators in the installed position are presented in figure 7. Both types of generators were mounted between the two flameholder gutter rings 12 inches downstream of the gutter trailing edge. This particular position was the only one tried, although other positions were expected to give somewhat different degrees of performance. The cylindrical-afterburner-shell length for both installations was $4\frac{1}{2}$ feet.

Instrumentation

Figure 8 is a schematic diagram of the afterburner indicating the location of the instrumentation stations. Total and static pressures were measured at stations 3, 4, 7, and 11. Afterburner-inlet temperature was measured at station 5. Other details of the instrumentation used at each station and associated recording equipment such as manometers and temperature recorders are given in reference 4.

Two of the four configuration changes investigated required modification of the reference-instrumentation layout. The inclined radial-gutter flameholder necessitated omission of the total-pressure survey rake at station 7, because the forward portion of the flameholder projected upstream into the diffuser passage. In the tapered-afterburner configuration, the total-pressure survey rake at station 11 was mounted just downstream of the conical nozzle so that the probe tips were located about 1/4 inch upstream of the nozzle-exit plane.

PROCEDURE

The operational procedure used with each configuration was essentially identical with that described in reference 4. Airflow rate was set by the inlet control valve, and the afterburner-inlet temperature was held constant at the desired value. Afterburner fuel was then injected and ignited. The exhaust pressure was maintained at a sufficiently low level to assure choking pressure ratio across the afterburner exhaust nozzle. A range of afterburner fuel-air ratios was covered by varying the afterburner fuel flow, while the afterburner-inlet velocity was maintained constant by adjusting the variable-area exhaust nozzle.

A slightly different procedure was followed in the case of the tapered-shell afterburner, wherein the fixed-area conical exhaust nozzle made the afterburner-inlet velocity a dependent function of afterburner temperature ratio (or fuel-air ratio). Consequently, a range of afterburner-inlet velocities at a given temperature ratio was established by using fixed-area nozzles of various sizes.

The fuel used throughout the investigation was MIL-F-5624A, grade JP-4, which has a lower heating value of 18,725 Btu per pound and a hydrogen-carbon ratio of 0.172.

Computational and data-reduction procedures were likewise identical to those outlined in reference 4. The actual combustion temperature used to define the combustion efficiency was calculated from the one-dimensional-flow continuity equation applied at the effective nozzle-exit area, where flow at sonic velocity was assumed to exist.

Afterburner-inlet flow conditions were computed from temperature measurements at station 5 and pressure measurements at station 7. In the case of the inclined radial-gutter flameholder, however, afterburner-inlet conditions were defined and compared with the reference configuration on the basis of pressure measurements at station 4 and temperature measurements at station 5.

A list of symbols used in the report is given in appendix A. Definitions and details of the calculation methods are presented in appendix B.

RESULTS AND DISCUSSION

The over-all combustion performance in an afterburner is contingent upon a mutual interaction of variables and upon the relative efficacy of each variable in the presence of other variables. Such tendencies and evidences of interaction for a conventional afterburner configuration are reported in reference 4. The configuration changes and the discussions which follow are intended to show the gross effects of geometrical

changes upon the over-all afterburner performance rather than to find the detailed mechanism which brings about the effects. Wherever existing evidence strongly indicates the cause of an effect, however, possible explanations are suggested.

The result of each configuration change is evaluated by comparison with the performance of the configuration of reference 4, thus providing a point of common reference for all configurations.

Reduced-Diameter Flameholder

Combustion efficiency. - Flame spreading is considered to be one of the factors governing combustion efficiency. Results of flame-spreading studies made in a rectangular duct are reported in reference 5. It is concluded in these studies that baffle width and blockage (up to 50 percent) had little effect on the rate of flame spreading, but that the degree of flame spreading depended on the distance the flame must spread from the center of a baffle to a wall or to a plane of symmetry. The shorter this distance, the greater the initial flame spreading. On the basis of these results, it may be surmised that a given level of efficiency can be obtained in a shorter afterburner when the degree of flame spreading is high; that is, when the distance between flameholders or between the flameholder and the wall is small.

Combustion efficiency of the reduced-diameter flameholder in the $3\frac{1}{2}$-foot afterburner is shown in figure 9. Data are presented for an afterburner-inlet temperature of 1660° R and pressures of 750 and 1800 pounds per square foot absolute in figures 9(a) and (b), respectively.

Comparison with the reference configuration shows a 25- to 30-percentage-point loss in efficiency at an afterburner-inlet velocity of 400 feet per second. (Distance between the afterburner wall and the outer gutter of the reduced-diameter flameholder was 4.375 in. compared with 2.875 in. in the reference configuration.) The loss in efficiency was thus consistent with the trends found in reference 5.

The combustion efficiency obtained in the $5\frac{1}{2}$-foot afterburner is shown in figure 10. At an afterburner-inlet velocity of 400 feet per second, the efficiency was about 13 and 7 percentage points lower than that of the reference configuration at pressures of 750 and 1800 pounds per square foot absolute, respectively. The increased afterburner length thus reduced the large efficiency loss encountered in the short $3\frac{1}{2}$-foot afterburner.

Lean blowout limits. - The lean blowout limits at the high and low ends of the pressure range at an afterburner-inlet temperature of 1660° R

are shown in figure 11. In the $3\frac{1}{2}$-foot afterburner, the limits of both the reduced-diameter flameholder and the reference configuration were about the same (fig. 11(a)).

In figure 11(b), the lean blowout limits of the $5\frac{1}{2}$-foot afterburner are shown to be poorer for the reference configuration, especially above afterburner-inlet velocities of about 500 feet per second. The limits of the reduced-diameter flameholder, however, were virtually unaffected by the increase in afterburner length from $3\frac{1}{2}$ to $5\frac{1}{2}$ feet. This is in agreement with reference 5, wherein it is reported that wide baffles and short afterburners are more stable. Long afterburners result in rough burning and pressure pulsations of considerable amplitude, which reduce afterburner stability.

No pressure measurements were made in the present investigation to determine the magnitude of oscillations. It is felt, however, that the wider gutters of the reduced-diameter flameholder (2 in. as compared with $1\frac{1}{2}$ in.) partially offset the tendency of the long afterburner to narrow the lean limits.

Another possible mechanism contributing to the narrower lean limits of the $5\frac{1}{2}$-foot reference afterburner is wall quenching. The smaller gap between the flameholder and the afterburner wall in the reference configuration makes the effects of wall quenching more probable and, hence, the lean limits poorer than in the reduced-diameter flameholder configuration. Results of detailed studies on quenching are reported in reference 1.

Pressure-loss coefficient. - The afterburner pressure-loss coefficients of the reduced-diameter flameholder configuration and the reference configuration at an afterburner-inlet temperature of 1660° R and pressure of 750 pounds per square foot absolute are shown in figure 12. Unless otherwise specified, the afterburner pressure-loss coefficient discussed throughout the report is defined as the drop in total pressure between the afterburner inlet and the effective nozzle exit divided by the dynamic head (total minus static pressures) at the afterburner inlet.

In both the $3\frac{1}{2}$-foot and $5\frac{1}{2}$-foot afterburners (figs. 12(a) and (b), respectively), the nonafterburning pressure-loss coefficients (afterburner temperature ratio = 1.0) were about the same as those of the reference configuration. Inasmuch as the projected blockage of both flameholders was equal, flameholder drag, and hence pressure loss, would be expected to be about the same.

[redacted]

Pressure-loss coefficients with afterburning generally increased with increasing afterburner temperature ratio and were somewhat higher in the reduced-diameter flameholder configuration than in the reference configuration. The decrease in pressure-loss coefficients with increasing velocity in the $3\frac{1}{2}$-foot afterburner (fig. 12(a)) is attributed to the relative magnitude and rate of increase of the afterburner-inlet dynamic head $P_7 - p_7$ compared with the afterburner pressure drop $P_7 - P_{12}$. A separate examination of these two factors showed that both the dynamic head and the pressure drop increased with increasing afterburner-inlet velocity, but that the dynamic head increased more rapidly. For instance, at an afterburner temperature ratio of 1.7, the pressure-loss coefficient decreased about 12 percent over a velocity range of 500 to 600 feet per second. The increase in dynamic head over the same velocity range was about 42 percent, whereas the pressure drop increased only 26 percent. The afterburner pressure-loss coefficients of the reduced-diameter flameholder in this operating range were 1.14 to 1.27 times those of the reference configuration.

In the $5\frac{1}{2}$-foot afterburner, the pressure-loss coefficient increased with increasing afterburner-inlet velocity and temperature ratio. Inasmuch as the afterburner-inlet velocities and, hence, the dynamic heads were of comparable magnitudes, the pressure drop in the $5\frac{1}{2}$-foot afterburner was obviously greater than that in the $3\frac{1}{2}$-foot afterburner. The cause of the large increase in pressure drop with 2 additional feet of afterburner length was not determined. At a temperature ratio of 1.8, the pressure-loss coefficient of the reduced-diameter flameholder increased 20 percent over a velocity range of 500 to 600 feet per second. Within this range of velocities, the pressure-loss coefficient of the reduced-diameter flameholder was about 1.05 times that of the reference configuration.

Summary. - Reducing the maximum flameholder diameter from 20 inches to 17 inches in a $3\frac{1}{2}$-foot-long afterburner reduced the combustion efficiency about 25 to 30 percentage points below that of the reference afterburner at an afterburner-inlet pressure of 750 pounds per square foot absolute and a velocity of 400 feet per second. At higher pressures and an afterburner length of $5\frac{1}{2}$ feet, the loss in efficiency at the same afterburner-inlet velocity was reduced to within 6 percentage points of the reference-configuration efficiency.

Lean blowout limits were about the same as those of the reference configuration and slightly better than those of the reference configuration above afterburner-inlet velocities of 500 feet per second in the $5\frac{1}{2}$-foot afterburner.

[redacted]

Pressure-loss coefficients in the $3\frac{1}{2}$- and $5\frac{1}{2}$-foot afterburners were about the same as those in the reference configuration during nonafterburning. Pressure-loss coefficients with afterburning were somewhat higher than those of the reference configuration and generally increased with increasing afterburner temperature ratio.

Inclined Radial-Gutter Flameholder

Combustion efficiency. - The inclined radial-gutter flameholder with a short cooling liner was operated in a $4\frac{1}{2}$-foot-long afterburner at an afterburner-inlet temperature of 1660° R. The combustion efficiency obtained is shown in figure 13. Afterburner operation was limited to a fuel-air ratio of about 0.055 because the uncooled portion of the afterburner shell overheated.

A comparison of efficiencies at low inlet pressures is shown in figure 13(a) for various diffuser-inlet (station 4) conditions, inasmuch as total-pressure surveys at the afterburner inlet (station 7) were not obtainable. The corresponding afterburner-inlet conditions of the reference configuration are listed in parentheses. Performance of the reference configuration extends only to its lean blowout fuel-air ratio of 0.040 to 0.035. The inclined radial-gutter flameholder, however, was operable at much leaner fuel-air ratios for all velocities. The combustion efficiency of the inclined radial-gutter flameholder between fuel-air ratios of 0.045 and 0.055 is equal to or only slightly lower than that of the reference configuration.

In general, as the fuel-air ratio was increased, the combustion efficiency reached a maximum at a fuel-air ratio of about 0.043 and then decreased with further increases in fuel-air ratio. It is suspected that either nonuniformity in fuel distribution, or a shift in flow pattern caused by the portion of the flameholder projecting upstream in the diffuser passage, or both, is responsible for this behavior. The presence of the cooling passage which permits about 14 percent of the flowing gas to be isolated from the mainstream may also affect the occurrence of the peak in efficiency.

The efficiencies at high inlet pressures are shown in figure 13(b). Reference-configuration data above an afterburner-inlet pressure of 1800 pounds per square foot absolute were not available; hence, the data at this pressure are used for a basis of comparison. At a diffuser-inlet velocity of 760 feet per second, the efficiencies of the two configurations showed approximately the same trends. At 600 feet per second, the efficiency of the inclined radial-gutter flameholder had a definite droop, thus lowering the efficiency 5 to 15 percentage points below that of the reference configuration.

The efficiency of the inclined radial-gutter flameholder with the long cooling liner is shown in figure 14. The long liner alleviated the overheating problem and extended the operable range to higher fuel-air ratios. The efficiency was equal to or lower than that of the reference configuration by 5 to 8 percentage points. The general level of efficiency near the maxima was not seriously affected by cooling-liner length. The apparent maxima occurred, however, at somewhat higher values of fuel-air ratio than in the short-liner configuration. Available static-pressure measurements indicated that, with the long liner and attendant pressure drop, the rate of gas flow in the cooling annulus was about one-fourth of that found in the short-liner cooling passage. Such changes in flow rate may have changed the flow pattern or fuel distribution sufficiently to affect the location of the maxima in efficiency.

The maximum values of combustion efficiency obtained with the inclined radial-gutter flameholder showed no significant improvement over those of the reference configuration. The basis of the flameholder design was to provide a circumferential flame seat both at the inner and outer radii, thus forming an annulus of unburned mixture surrounded by flame surfaces interconnected by radial gutters. The lack of a significant improvement in combustion efficiency may be due to one or all of three possible reasons: (1) The flameholder projecting into the diffuser passage may have stratified an otherwise uniform fuel-air distribution; (2) flame propagation between adjacent inclined radial gutters was not complete because of the high-velocity flow field; (3) there was not sufficient time for the combustion process to go to completion after the fuel-air mixture entered the flame-reaction zone. Which of these factors was controlling could not be determined from the type of tests made in the present investigation.

Lean blowout limits. - Lean blowout data of the inclined radial-gutter flameholder with both cooling liners are shown in figure 15. Reference-configuration blowout data to match the 880-pound-per-square-foot-absolute diffuser-inlet pressure condition were unavailable. The limits at a pressure of approximately 800 pounds per square foot absolute are therefore used as a basis of comparison in figure 15(a). The corresponding afterburner-inlet velocities of the reference configuration are shown by an inserted scale to the right of the figure.

In comparison with the reference configuration, the lean limits with the short liner (fig. 15(a)) were considerably better than those with the long liner. This is consistent with the suppositions made earlier regarding efficiency. Peaks in efficiency at low fuel-air ratios followed by decreasing efficiency at higher fuel-air ratios indicate the presence of locally rich mixture regions. Such locally rich regions continue burning to leaner over-all fuel-air ratios and thus improve the lean limits. Changes in flow caused by a long liner may thus affect the mass velocity or fuel-air distribution sufficiently to move the lean

limits to higher over-all fuel-air ratios. A geometrical factor also contributing to better lean limits regardless of flow or mixture distribution was the greater width of the inclined radial gutter.

The lean blowout limits at the high diffuser-inlet pressure level are shown in figure 15(b) with values of the diffuser-inlet pressure for each point tabulated. The limits of the reference configuration at the nearest matching pressure of approximately 1900 pounds per square foot absolute are shown for comparison. The inclined radial-gutter flameholder had limits that were better by about 0.01 fuel-air ratio. This improvement may be attributed to the wider gutters. No large effect of cooling-liner length was apparent at this pressure level.

Lean blowout limits of a baffle-type combustor can be greatly improved by a fuel-injection system that maintains a locally rich fuel-air mixture around the flameholder. Comparisons of lean blowout limits to show relative merits of different configurations are not completely fair unless a uniform fuel-air mixture is assured in both cases. On the basis of results found here and in previous investigations, such as reference 8, it may be concluded that at afterburner-inlet flow conditions such as low pressure and high velocity, where differences in flame stability are most noticeable, a flameholder with wide gutters exhibits greater stability.

Pressure-loss coefficient. - As mentioned previously, pressure instrumentation at station 7 normally used in evaluating afterburner pressure loss could not be installed in this case (see fig. 4(b)). The over-all afterburner pressure-loss coefficient is therefore defined as the loss in total pressure between stations 4 and 12 divided by the dynamic head (total minus static pressures) at station 4. The pressure-loss coefficients of the inclined radial-gutter flameholder configuration and the comparative reference configuration thus include the diffuser loss. The pressure-loss coefficient is shown in figure 16 for a range of diffuser-inlet pressures from 820 to 2000 pounds per square foot absolute, which corresponds to afterburner-inlet pressures from 780 to 1900 pounds per square foot in the reference configuration. At a diffuser-inlet velocity of 850 feet per second, the loss coefficient with the short liner was 1.8 to 2.6 times larger than that of the reference configuration, depending on the afterburner temperature ratio. The higher pressure loss of the inclined radial-gutter flameholder may be attributed to larger flameholder drag caused by higher projected blockage area and the flat-plate shape of the radial-gutter elements.

The pressure-loss coefficient with the long liner at the same diffuser-inlet velocity was 2.5 to 3.8 times that of the reference configuration. The exact reasons for the larger pressure loss with the long liner are not known, although the change in cooling-annulus gas flow is felt to be the primary cause. As stated previously, flow in the cooling annulus with the long liner was about one-fourth that in the short-liner

configuration. This reduction in flow may have affected the formation of a vortex sheet along the outer gutter, thus modifying the vorticity and turbulence in the wake region and giving rise to larger drag or pressure losses. The flow process is visualized schematically in the accompanying sketch:

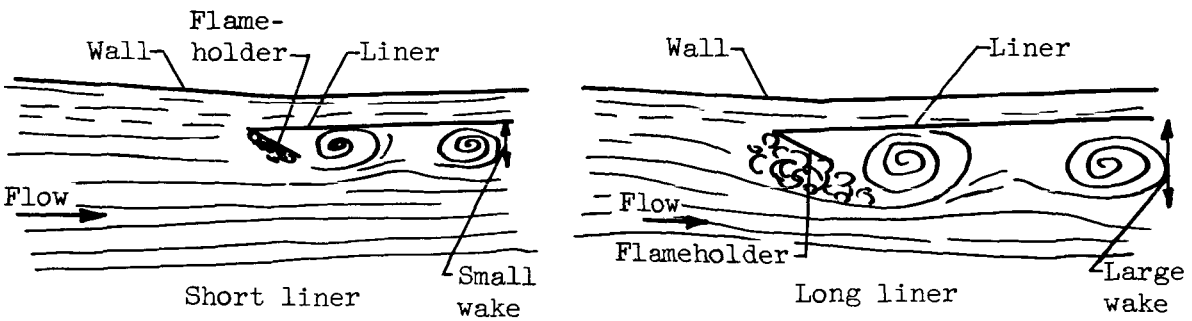

The flow rate through the short cooling liner was only about 14 percent of the total afterburner gas flow. A corresponding increase in gas flow through the flameholder region from even a complete blockage of the cooling annulus cannot be expected to cause such a large observed increase in pressure loss unless a major change in the flow process, such as the one illustrated, has occurred.

Summary. - The inclined radial-gutter flameholder with either the short or the long cooling liner operated at a combustion efficiency equal to that of the reference configuration or lower by as much as 5 to 15 percentage points. The efficiency curves exhibited a droop as the fuel-air ratio increased. This droop was somewhat less with the long-liner configuration, and the peak occurred at higher fuel-air ratios than in the short-liner configuration.

Lean blowout limits were considerably better in the short-liner configuration at the low diffuser-inlet pressure level. At the higher pressure level, both the short-liner and long-liner configurations were better than the reference configuration by about 0.01 fuel-air ratio.

With the short-liner configuration, the over-all afterburner pressure-loss coefficient (including the diffuser) at a diffuser-inlet velocity of 850 feet per second was 1.8 to 2.6 times larger than that of the reference afterburner. With the long liner, the pressure-loss coefficient increased 2.5 to 3.8 times that of the reference configuration.

Tapered-Shell Afterburner

Combustion efficiency. - The curves shown in figure 17 are cross plots of combustion data at an afterburner fuel-air ratio of 0.055 compared with similar cross plots of data from the reference configuration

having an equal afterburner volume. (The length of the cylindrical, or reference, afterburner having the same volume as the tapered afterburner was computed to be 36 in.)

Comparisons of efficiency at afterburner-inlet pressure levels of 750, 1270, and 1800 pounds per square foot absolute are shown in figures 17(a), (b), and (c), respectively. At each pressure level, where possible, curves of combustion efficiency are shown for the three afterburner-inlet temperatures. A direct comparison of efficiency at the cross-plotted fuel-air ratio of 0.055 was possible only at afterburner-inlet velocities near 400 feet per second. The fixed geometry of the largest afterburner-exit area (tapered shell with no exhaust nozzle) prevented simulation of a higher afterburner-inlet velocity at this fuel-air ratio and existing temperature ratio.

Although the results are not conclusive, the combustion efficiencies of the two configurations near an afterburner-inlet velocity of 400 feet per second appeared to agree within 5 percentage points. However, the efficiency of the tapered afterburner appeared to decrease more rapidly with increasing afterburner-inlet velocity. This is possibly due to the higher flow velocities in the burning zone of the tapered afterburner as the flow area progressively decreased. Such increases in velocities are detrimental to flame propagation and hence detrimental to combustion efficiency.

A similar comparison is made in reference 3, in which it is also shown that the combustion efficiencies of the tapered and cylindrical afterburners showed better agreement when compared on a basis of equal afterburner volume rather than on equal length. Afterburner volume in either case was determined as that volume existing between two cross-sectional planes passing through the trailing edge of the flameholder gutters and the effective nozzle exit. The comparison in reference 3, however, is limited to two available data points.

Lean blowout limits. - The lean blowout limits of the tapered afterburner and the cylindrical afterburner of equal volume are shown in figure 18. Limits at afterburner-inlet pressure levels of 750, 1270, and 1800 pounds per square foot absolute are shown in figures 18(a), (b), and (c), respectively. At each pressure level, data are shown for two afterburner-inlet temperatures. In all cases, higher inlet temperature shifted the lean limit to lower values of fuel-air ratio. Available data are not extensive enough to compare directly the limits over a wide range of afterburner-inlet velocities. The lean blowout limits of the tapered afterburner, however, narrowed more rapidly with increasing afterburner-inlet velocity than those of the reference configuration.

Afterburner pressure-loss coefficient. - Pressure-loss coefficients in the tapered afterburner and in the cylindrical afterburner of equal

[redacted]

volume are shown in figure 19 over a range of afterburner-inlet pressures from 750 to 1800 pounds per square foot absolute for various values of afterburner temperature ratio. With no combustion (temperature ratio = 1.0), the pressure-loss coefficients were about equal for both configurations. Losses in this case were primarily due to flameholder drag. Because the same flameholder was used in both cases, the flameholder drag was practically identical.

With combustion, the pressure-loss coefficient in the tapered afterburner was about 1.2 times that of the cylindrical afterburner. The increase in pressure-loss coefficient per increment of temperature rise was also greater in the tapered afterburner. The higher pressure-loss coefficient in the tapered afterburner may be attributed to burning and heat addition at the higher flow velocities that existed along the afterburner as the flow area progressively decreased.

Summary. - The combustion efficiency of the tapered-shell afterburner at a fuel-air ratio of 0.055 and an afterburner-inlet velocity of about 400 feet per second was within 5 percentage points of the efficiency of a cylindrical afterburner having an equal volume. The efficiency of the tapered-shell afterburner, however, had a tendency to degenerate more rapidly with increasing afterburner-inlet velocity.

Lean blowout limits of the two afterburners shifted to lower values of fuel-air ratio as afterburner-inlet temperature increased. The limits of the tapered afterburner narrowed more rapidly with increasing afterburner-inlet velocity.

Afterburner pressure-loss coefficients with no combustion were the same in both afterburners, but the pressure-loss coefficient with combustion in the tapered afterburner was about 1.2 times that of the cylindrical afterburner.

Turbulence Generators

Some previous studies of flame stabilization and flame spreading from baffles in a high-velocity gas stream have shown that increasing the approach-stream turbulence increases the width of spreading flames but narrows the stability limits. For instance, higher initial rates of flame spreading with the introduction of small-scale turbulence are indicated in reference 5; whereas a 15-percent decrease in stability limits as approach-stream turbulence intensity increased from 0.4 to 1.85 percent is reported in reference 8.

The intended purpose of the present investigation was to employ turbulence generators so as to promote turbulence ahead of the flame front and thus increase the rate of flame spreading and combustion

efficiency, yet avoid turbulence ahead of the flameholder and thus avoid reductions in stability limits. Two types of turbulence generators were used; both types of generators were mounted 12 inches downstream of the flameholder on a line midway between the two gutter rings.

Vortex generators. - The vortex-type turbulence generator was mounted in a $4\frac{1}{2}$-foot cylindrical afterburner and operated at an afterburner-inlet temperature of 1660° R. The combustion efficiency of this configuration at an afterburner-inlet pressure of 750 pounds per square foot absolute and a range of afterburner-inlet velocities is shown in figure 20. At velocities of 500 and 550 feet per second, the efficiency was $3\frac{1}{2}$ to $8\frac{1}{2}$ percentage points lower than that of the reference configuration over an afterburner fuel-air ratio range from 0.045 to 0.0675. At an afterburner-inlet velocity of 400 feet per second and a fuel-air ratio of 0.0675, the combustion efficiency was about the same as that of the reference configuration.

A direct comparison with the results of reference 7 cannot be made because of differences in flameholder details and operating conditions. The improvement in efficiency gained by adding vortex generators 13 inches downstream of the flameholder is reported to be small - in the order of 0.5 to 1.0 percentage point. However, as much as 12-percentage-point improvement in combustion efficiency was obtained in the afterburner of reference 7 as the spacing between the flameholder and the vortex generators was reduced from 13 to 2 inches.

The lean blowout limits are shown in figure 21 at three levels of afterburner-inlet pressure. The lean limits at a pressure of 750 pounds per square foot absolute were noticeably lower than those of the reference configuration but only imperceptively so at the other two pressure levels.

The afterburner pressure-loss coefficient at an afterburner-inlet pressure of 750 pounds per square foot absolute is shown in figure 22. Nonafterburning pressure-loss coefficients were only slightly higher while afterburning pressure-loss coefficients at all afterburner temperature ratios were considerably higher for the vortex generator than for the reference configuration. At the higher afterburner temperature ratios, the pressure-loss coefficient increased very sharply with increasing afterburner-inlet velocity above 400 feet per second. This rapid rise may be due to strong flame-generated turbulence caused by heat addition and flow acceleration in the presence of high initial turbulence. Losses from such a source conceivably can be higher than those in the case of no heat addition. At a temperature ratio of 1.8, the pressure-loss coefficient was 1.3 and 2.1 times that of the reference configuration at afterburner-inlet velocities of 400 and 600 feet per second,

respectively. At a temperature ratio of 1.0, the pressure-loss coefficient at the corresponding afterburner-inlet flow conditions was only 1.3 and 1.9 times greater than that of the reference configuration.

Radial-vane mixer. - The combustion efficiency obtained with the second type of turbulence generator, the radial-vane mixer, is shown in figure 23. Afterburner length and afterburner-inlet conditions were identical with those of the previous configuration. In general, the combustion efficiency was poorer than that of the reference configuration by about 5 to 17 percentage points.

Lean blowout limits, as shown in figure 24, were inferior to the reference configuration by a maximum of about 0.004 fuel-air ratio at an afterburner-inlet velocity of 475 feet per second and a pressure of 750 pounds per square foot absolute.

The afterburner pressure-loss coefficient (fig. 25) at an afterburner temperature ratio of 1.8 was 1.5 to 1.9 times that of the reference configuration at afterburner-inlet velocities of 400 and 600 feet per second over a pressure range from 750 to 1270 pounds per square foot absolute. In contrast to the behavior of the vortex generator, the pressure-loss coefficient of the vane mixer during afterburning did not rise quite as rapidly with increasing afterburner-inlet velocity.

Summary. - Turbulence generators of both types used in this investigation operated with a combustion efficiency equal to or lower than that of the reference configuration. Only one position of the turbulence generators relative to the flameholder was used. In reference 7 a 12-percentage-point improvement in combustion efficiency is reported as the spacing between the flameholder and the turbulence generators was reduced from 13 to 2 inches. Close spacing may have improved the efficiency in the present investigation also.

Lean blowout limits were slightly poorer than those of the reference configuration. The afterburner pressure-loss coefficient was as much as twice that of the reference configuration at an afterburner-inlet velocity of 600 feet per second.

Results indicate that considerable turbulence was generated but with no apparent improvement in combustion efficiency. The scale of turbulence generated may have been sufficiently large to disturb the flow excessively and to disrupt the flame front, thus creating a negative effect on flame spreading. The possibility exists, however, that, at some optimum combination of generator spacing and afterburner length, the efficiency with the turbulence generators may be higher than that of the corresponding reference configuration.

[redacted]

SUMMARY OF RESULTS

The results of an experimental investigation conducted in a 25.75-inch-diameter simulated-afterburner test rig to evaluate the combustion performance of (1) a V-gutter flameholder with the maximum gutter-ring diameter 3 inches less than that of a reference configuration, but with equal projected blockage; (2) an inclined radial-gutter flameholder; (3) a tapered-shell afterburner; and (4) a V-gutter flameholder with turbulence generators added may be summarized as follows:

1. Reducing the maximum flameholder diameter in a $3\frac{1}{2}$-foot-long afterburner seriously decreased the combustion efficiency below that of the reference configuration. In a $5\frac{1}{2}$-foot-long afterburner, the combustion efficiency obtained with the same flameholder when operated at high afterburner-inlet pressures was almost equal to that of the reference configuration. Lean blowout limits at high velocities in the long afterburner were slightly better than the limits of the reference configuration. The nonafterburning pressure-loss coefficients were about the same for both configurations. Pressure-loss coefficients with afterburning were higher than those of the reference configuration and generally increased with increasing afterburner temperature ratio.

2. The inclined radial-gutter flameholder with either the short or the long cooling liner operated in a $4\frac{1}{2}$-foot-long afterburner gave equal or slightly lower combustion efficiency, better lean blowout limits, and a higher pressure-loss coefficient than those of the reference configuration.

3. The performance of a tapered-shell V-gutter afterburner compared with that of a similar cylindrical afterburner having an equivalent afterburner volume showed that combustion efficiencies at identical operating conditions were about equal, but that the efficiency of the tapered afterburner appeared to degenerate more rapidly with increasing afterburner-inlet velocity. Lean blowout limits similarly narrowed more rapidly with increasing velocity. Afterburner pressure-loss coefficient during afterburning was higher, but nonafterburning pressure-loss coefficient was the same, as in the cylindrical afterburner.

4. Two types of turbulence generators mounted, in each case, 12 inches downstream of the flameholder and operating in a $4\frac{1}{2}$-foot-long afterburner gave combustion efficiency equal to or lower than that of the conventional V-gutter configuration taken as reference. Lean blowout limits were slightly poorer, and the pressure-loss coefficient was much

[redacted]

higher, than those of the reference configuration during afterburning at high afterburner-inlet velocities.

Lewis Flight Propulsion Laboratory
National Advisory Committee for Aeronautics
Cleveland, Ohio, March 11, 1957

APPENDIX A

SYMBOLS

A	exhaust-nozzle-throat area, sq ft
f/a	fuel-air ratio
g	acceleration due to gravity, 32.17 ft/sec^2
m	mass flow, slugs/sec
P	total pressure, lb/sq ft abs
p	static pressure, lb/sq ft abs
R	gas constant, 53.35 ft-lb/(lb)(^oR)
T	total temperature, ^oR
V	velocity, ft/sec
w	weight flow, lb/sec
η	combustion efficiency

Subscripts:

AB	afterburner
a	air
eff	effective
f	fuel
g	gas
id	ideal
o	over all
p	preheater
st	stoichiometric
u	available air

3	upstream of airflow measuring screen, mixing-chamber outlet
4	diffuser inlet
5	spray-bar inlet
6	fuel injection
7	afterburner inlet, diffuser exit
11	exhaust-nozzle inlet
12	effective exhaust-nozzle exit

APPENDIX B

METHODS OF CALCULATION

Air Flow

The air flow was determined from the measured pressure drop across the diffuser-inlet screen calibrated against a series of fixed-area exhaust nozzles of known flow coefficient. Suitable corrections were made for the preheater fuel flow included in the gas flow during the calibration process.

Gas Flow

The afterburner gas flow was determined by summing up the measured air and fuel flows:

$$w_g = w_a + w_{f,p} + w_{f,AB} \tag{B1}$$

Velocity

The velocity at the diffuser inlet and exit (or afterburner inlet) was computed from measured total and static pressures and the total temperature by use of the one-dimensional-flow parameters of reference 9, which are a function of total- to static-pressure ratio for a given ratio of specific heats:

$$V_{4 \text{ or } 7} = \left(\frac{V}{\sqrt{gRT}}\right)_{4 \text{ or } 7} \sqrt{gRT_5} \tag{B2}$$

The temperatures T_4 and T_7 were assumed equal to T_5, and the ratio of specific heats was assumed to be 1.3.

Fuel-Air Ratio

The various fuel-air ratios were defined and computed as follows:

$$\text{Preheater fuel-air ratio } (f/a)_p = \frac{w_{f,p}}{w_a} \tag{B3}$$

$$\text{Afterburner total fuel-air ratio } (f/a)_{AB} = \frac{w_{f,AB}}{w_a} \tag{B4}$$

$$\text{Over-all fuel-air ratio } (f/a)_o = \frac{w_{f,p} + w_{f,AB}}{w_a} \tag{B5}$$

$$\text{Afterburner available air } (f/a)_{AB,u} = \frac{\text{Total unburned fuel to afterburner}}{\text{Total available air to afterburner}}$$

$$= \frac{w_{f,AB} + (w_{f,p} - w_{f,p,id})}{w_a - \frac{w_{f,p,id}}{(f/a)_{st}}} \tag{B6}$$

where $(w_{f,p} - w_{f,p,id})$ is the fuel not burned in the preheater and chargeable to the afterburner, and $\frac{w_{f,p,id}}{(f/a)_{st}}$ is the air reacted in the preheater. Dividing the numerator and denominator of equation (B6) by w_a gives

$$(f/a)_{AB,u} = \frac{(f/a)_{AB} + (f/a)_p - (f/a)_{p,id}}{1 - \frac{(f/a)_{p,id}}{0.0676}} \tag{B7}$$

where 0.0676 is the stoichiometric fuel-air ratio for the fuel used. But, since

$$(f/a)_{AB} + (f/a)_p = (f/a)_o$$

equation (B7) becomes

$$(f/a)_{AB,u} = \frac{(f/a)_o - (f/a)_{p,id}}{1 - \frac{(f/a)_{p,id}}{0.0676}}$$

The ideal preheater fuel-air ratio $(f/a)_{p,id}$ was obtained from reference 10.

Combustion Temperature

The total temperature of the exhaust gas was computed from the one-dimensional-flow continuity equation applied at the effective exhaust-nozzle-exit area where sonic-flow velocity was assumed to exist:

$$T_{12} = \frac{g}{R}\left[\left(\frac{m\sqrt{gRT}}{PA}\right)_{12}\left(\frac{P_{12}A_{eff}}{w_g}\right)\right]^2$$

[redacted]

where $\left(\frac{m\sqrt{gRT}}{PA}\right)_{12}$ is the dimensionless total-pressure parameter of reference 9 for critical flow at the exhaust nozzle.

Afterburner Combustion Efficiency

The afterburner combustion efficiency was defined as the ratio of the actual afterburner temperature rise to the theoretical temperature rise:

$$\eta_{AB} = \frac{T_{12} - T_5}{T_{12,id} - T_5}$$

Values of $T_{12,id}$ were obtained by the method of reference 10.

REFERENCES

1. Fuels and Combustion Research Division: Adaptation of Combustion Principles to Aircraft Propulsion. Vol. I. Basic Considerations in the Combustion of Hydrocarbon Fuels with Air. NACA RM E54I07, 1955.

2. Fuels and Combustion Research Division: Adaptation of Combustion Principles to Aircraft Propulsion. Vol. II. Combustion in Air-Breathing Jet Engines. NACA RM E55G28, 1956.

3. Lundin, Bruce T., Gabriel, David S., and Fleming, William A.: Summary of NACA Research on Afterburners for Turbojet Engines. NACA RM E55L12, 1956.

4. King, Charles R.: Experimental Investigation of Effects of Combustion-Chamber Length and Inlet Total Temperature, Total Pressure, and Velocity on Afterburner Performance. NACA RM E57C07, 1957.

5. Petrein, Richard J., Longwell, John P., and Weiss, Malcolm A.: Flame Spreading from Baffles. Bumblebee Ser., Rep. No. 234, Esso Res. and Eng. Co., June 1955. (Contract NOrd 9233 with Bur. Ord., Dept. Navy.)

6. Rayle, Warren D., and Koch, Richard G.: Design of Combustor for Long-Range Ram-Jet Engine and Performance of Rectangular Analog. NACA RM E53K13, 1954.

7. Prince, William R., Velie, Wallace W., and Braithwaite, Willis M.: Full-Scale Evaluation of Some Flameholder Design Concepts for High-Inlet-Velocity Afterburners. NACA RM E56D10, 1956.

8. Williams, G. C., Hottel, H. C., and Scurlock, A. C.: Flame Stabilization and Propagation in High Velocity Gas Streams. Third Symposium on Combustion and Flame and Explosion Phenomena, The Williams & Wilkins Co., 1949, pp. 21-40.

9. Turner, L. Richard, Addie, Albert N., and Zimmerman, Richard H.: Charts for the Analysis of One-Dimensional Steady Compressible Flow. NACA TN 1419, 1948.

10. Huntley, S. C.: Ideal Temperature Rise Due to Constant-Pressure Combustion of a JP-4 Fuel. NACA RM E55G27a, 1955.

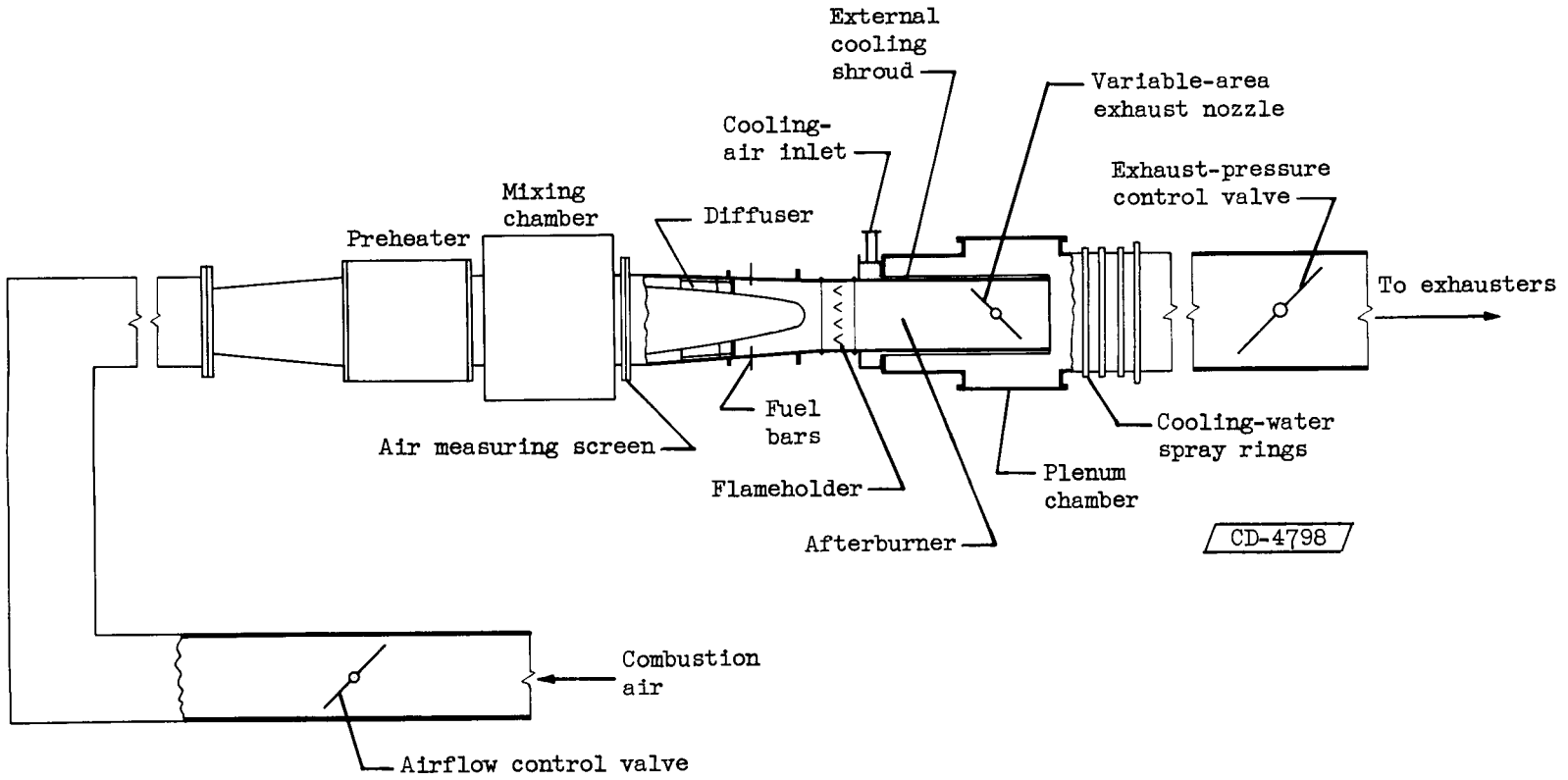

Figure 1. - Schematic layout of simulated-afterburner test rig.

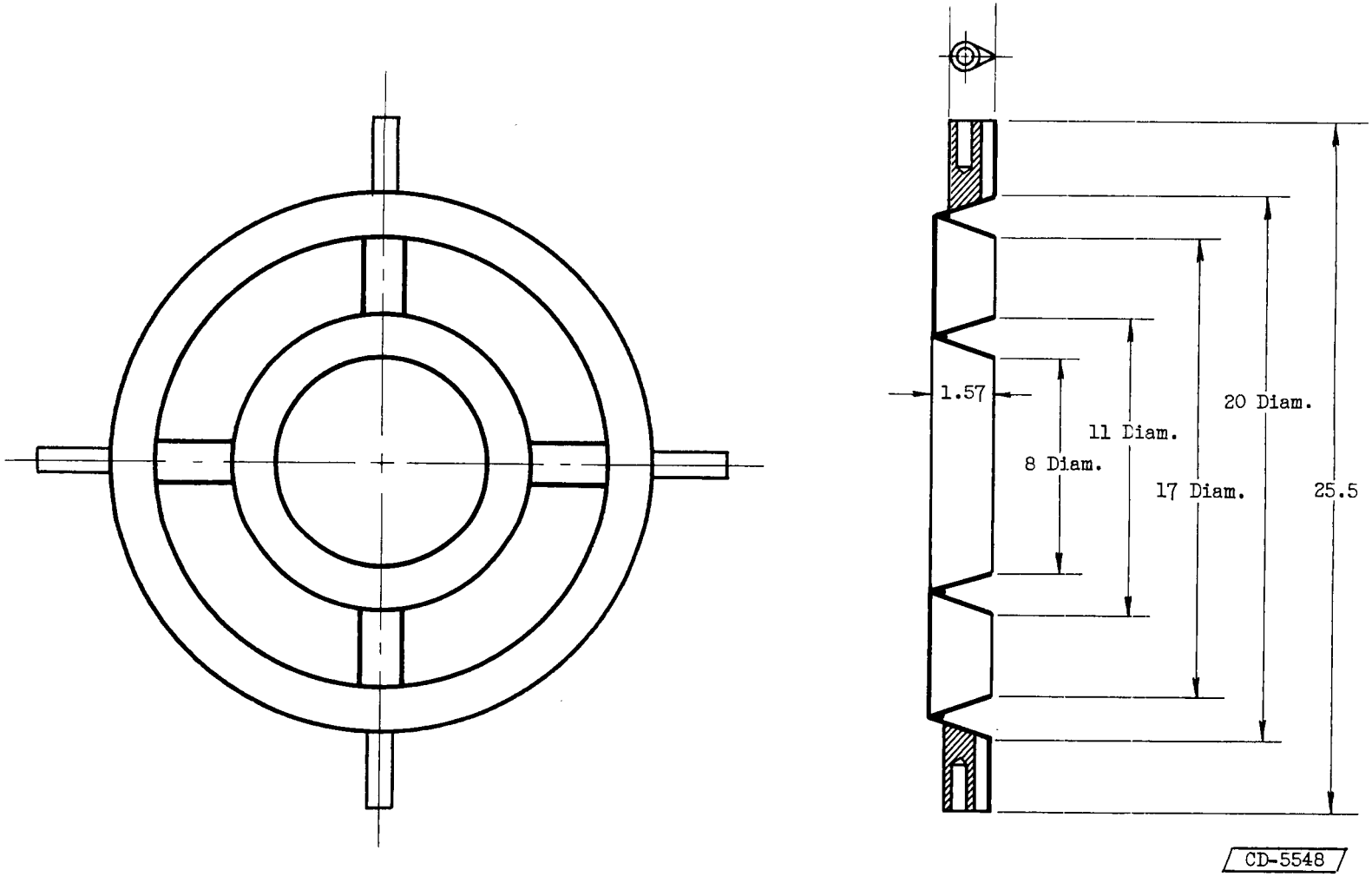

Figure 2. - Reference-configuration flameholder. Projected blockage, 29.6 percent of combustion-chamber cross-sectional area. (All dimensions in inches.)

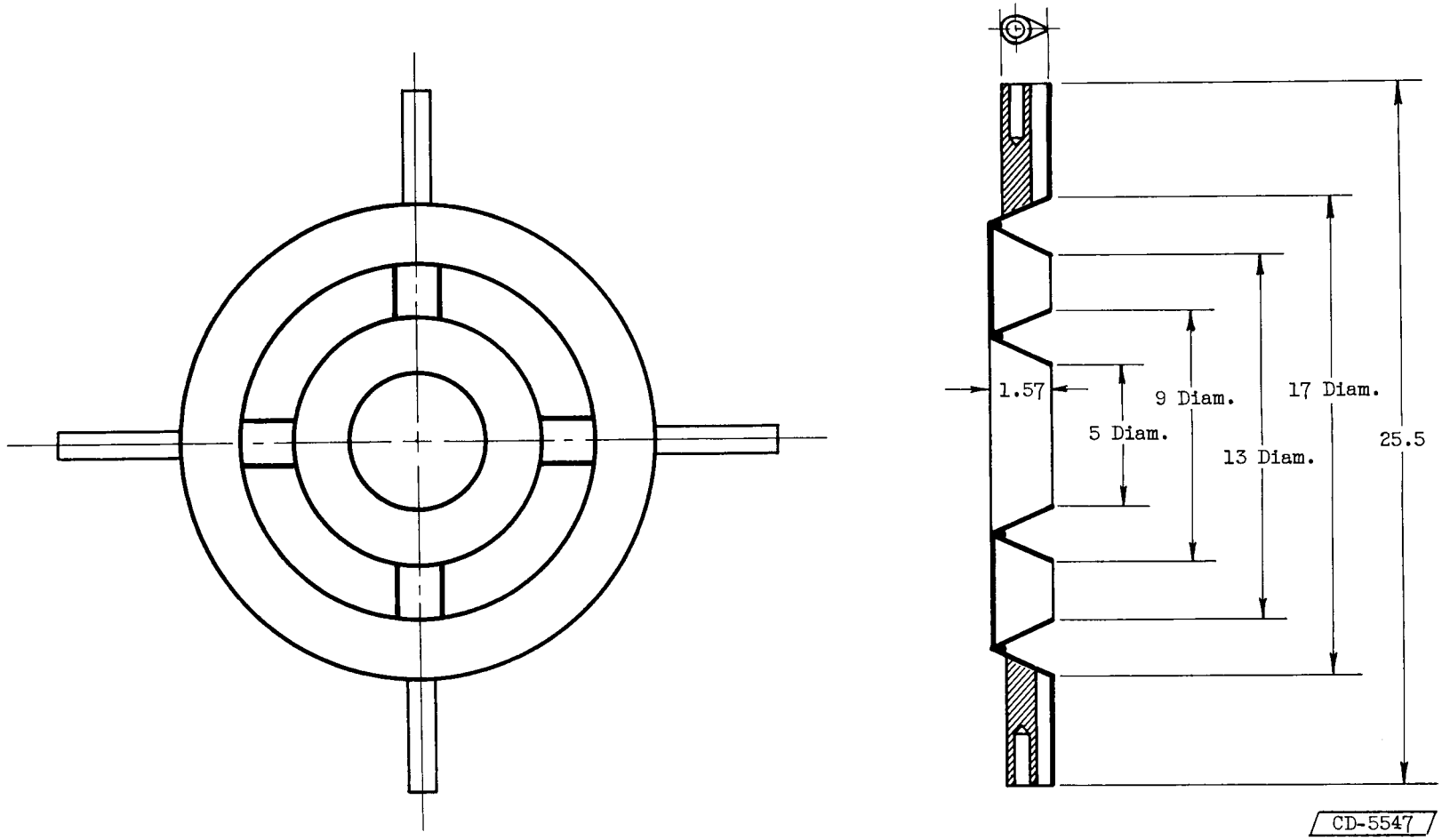

Figure 3. - Reduced-diameter flameholder. Projected blockage, 29.6 percent of combustion-chamber cross-sectional area. (All dimensions in inches.)

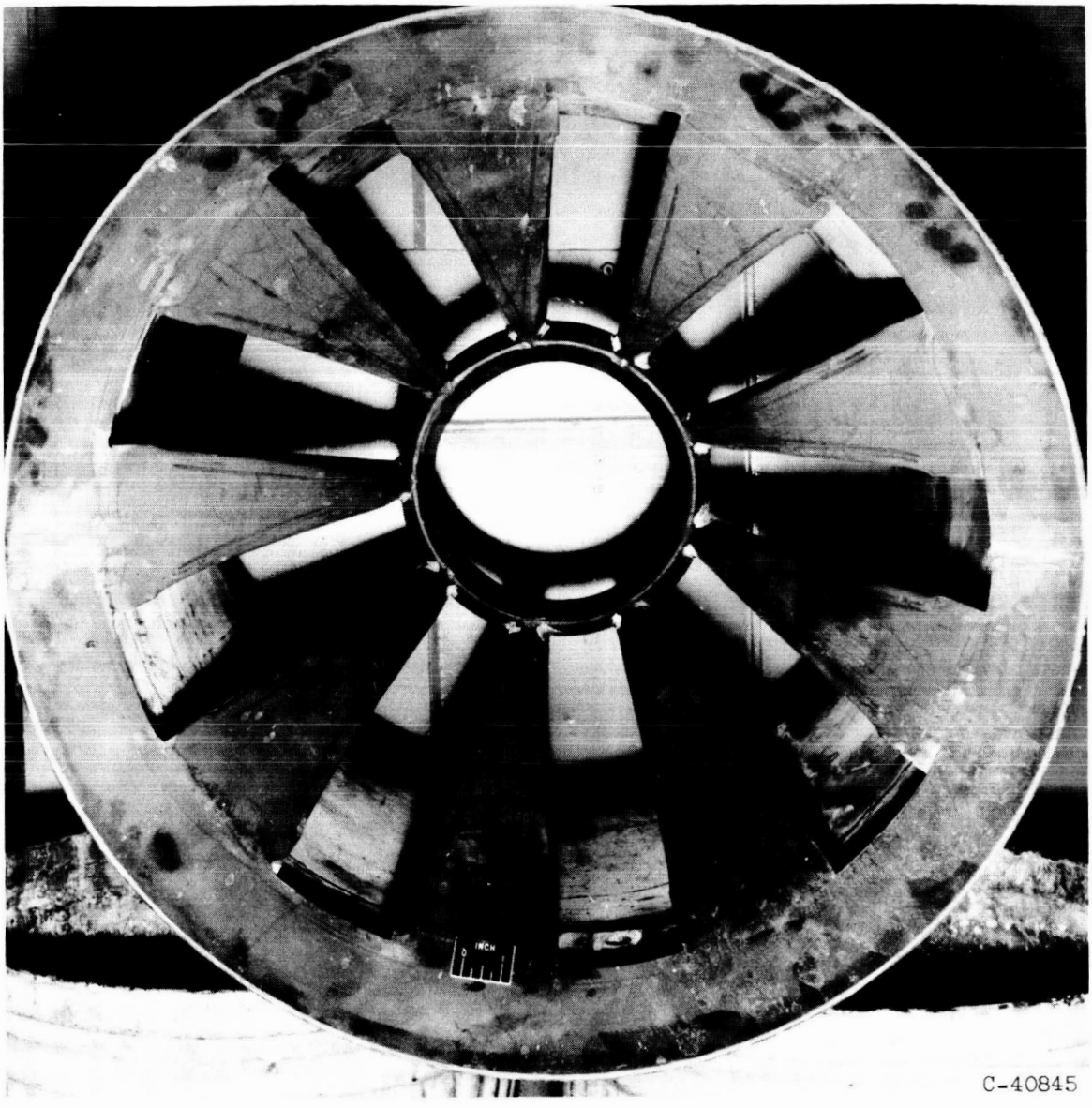

(a) Front view.

Figure 4. - Inclined radial-gutter flameholder.

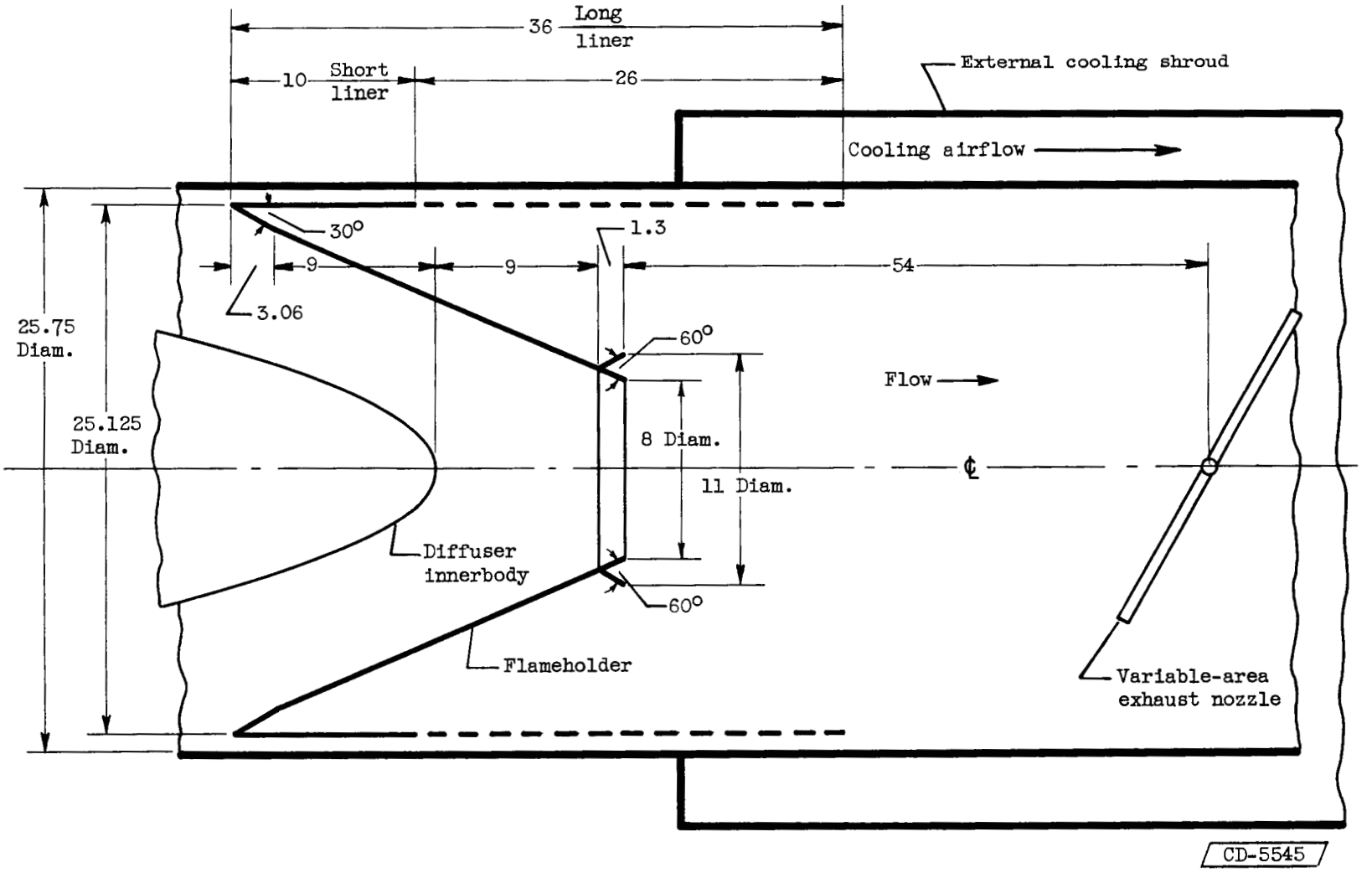

(b) Installed view. (All dimensions in inches.)

Figure 4. - Concluded. Inclined radial-gutter flameholder.

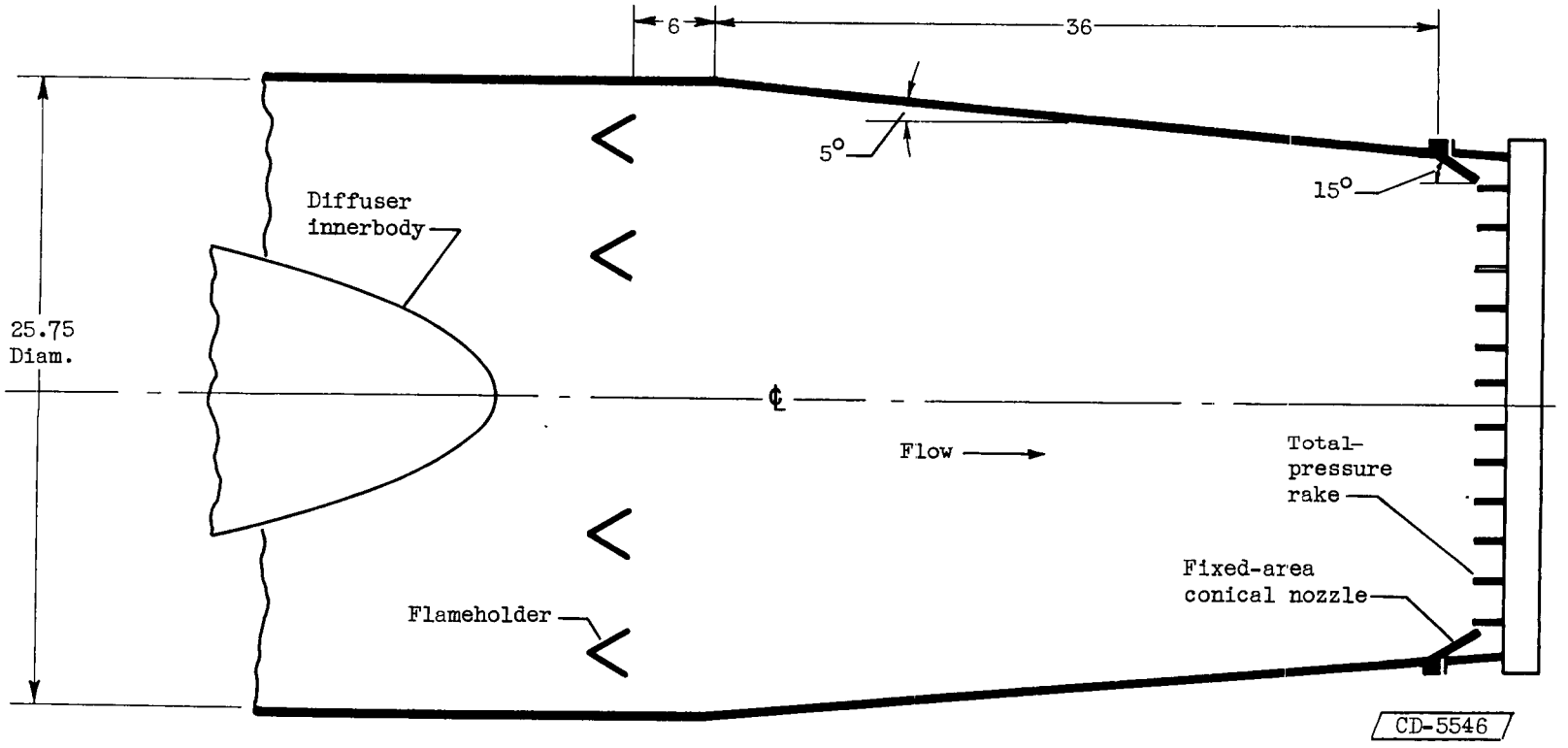

Figure 5. - Tapered-shell afterburner. (All dimensions in inches.)

(a) Vortex generator. (b) Radial-vane mixer.

Figure 6. - Turbulence generators.

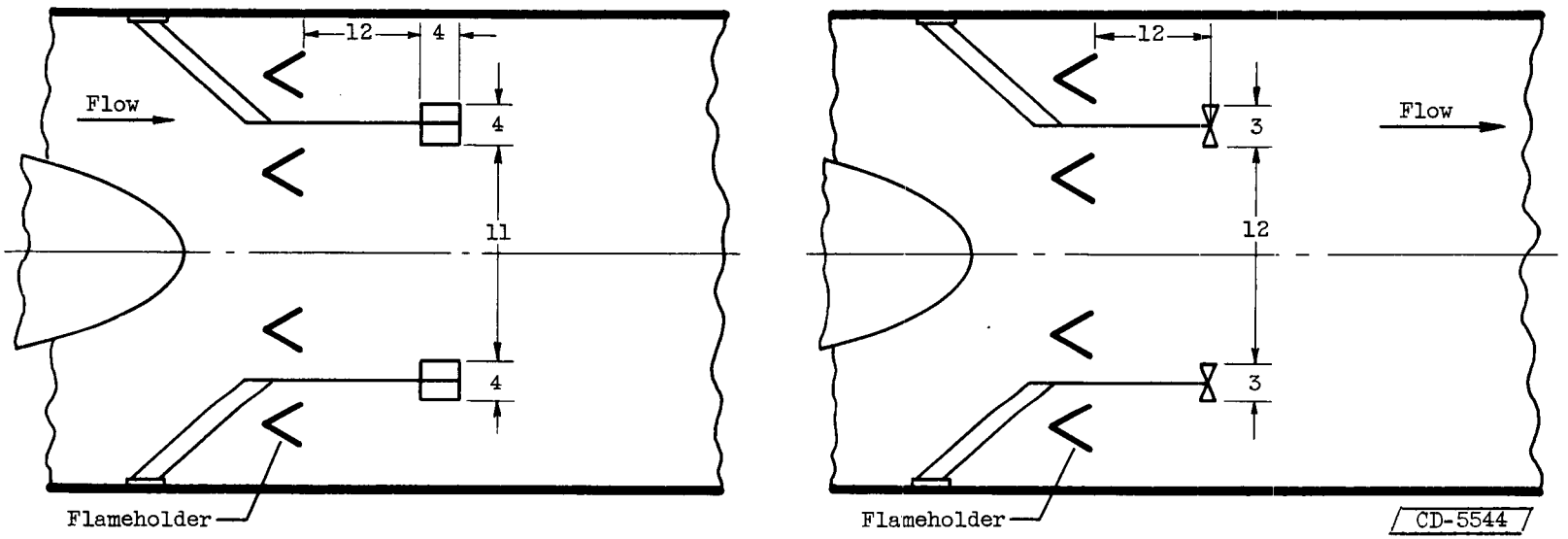

(a) Vortex generator.

(b) Radial-vane mixer.

Figure 7. - Turbulence generators installed. (All dimensions in inches.)

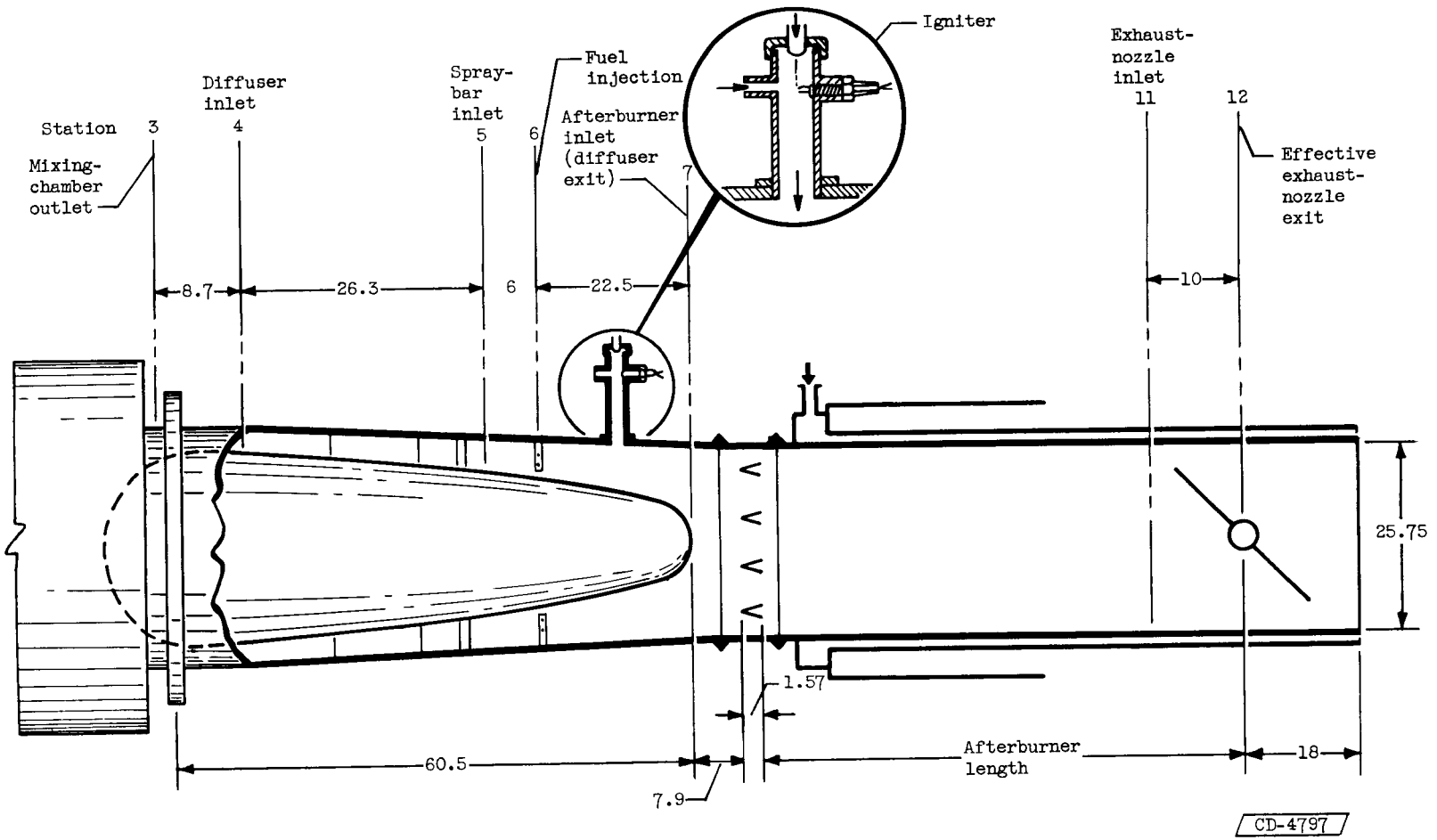

Figure 8. - Instrumentation stations. (All dimensions in inches.)

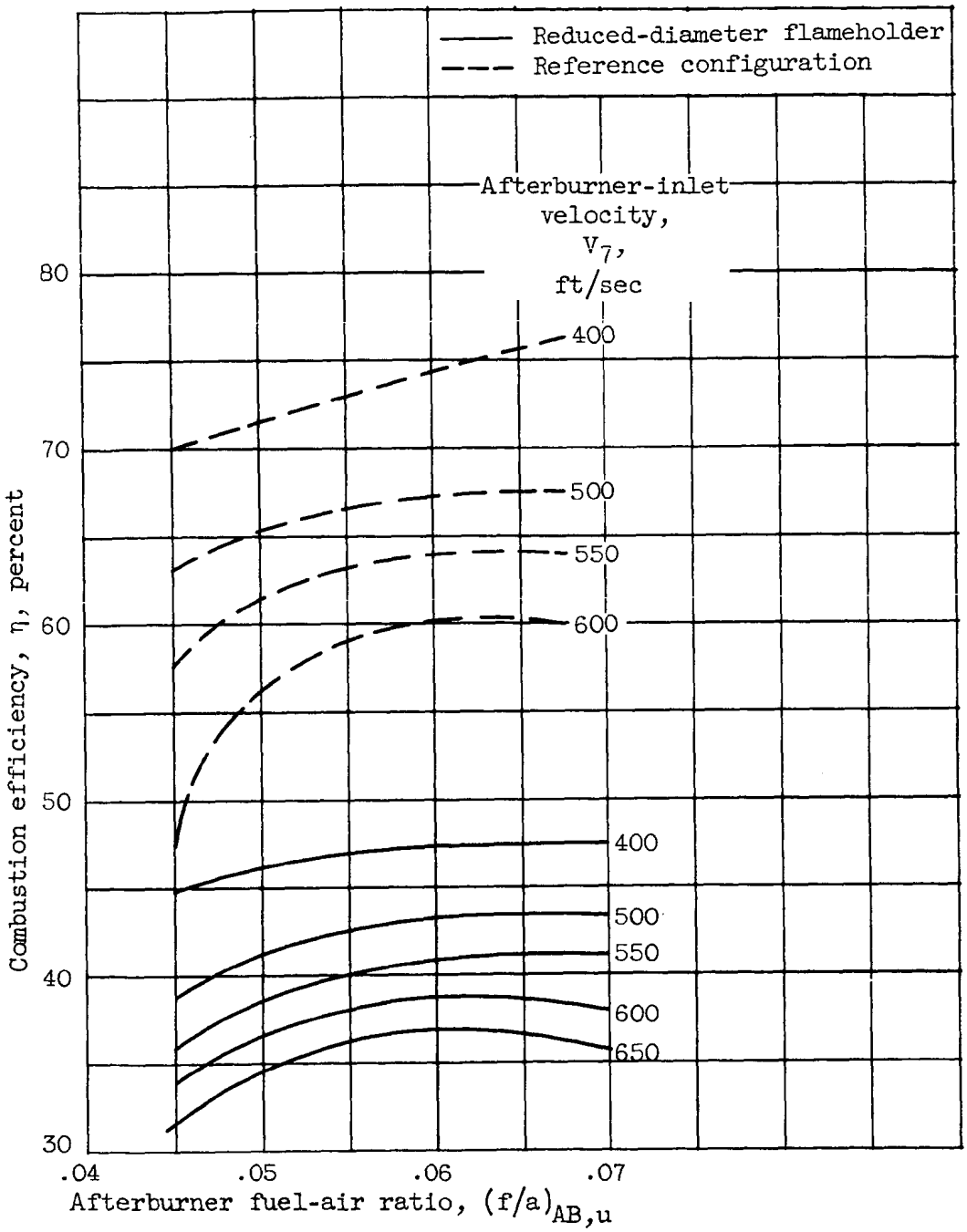

(a) Afterburner-inlet pressure, 750 pounds per square foot absolute.

Figure 9. - Combustion efficiency of reduced-diameter flameholder in $3\frac{1}{2}$-foot afterburner. Afterburner-inlet temperature, 1660° R.

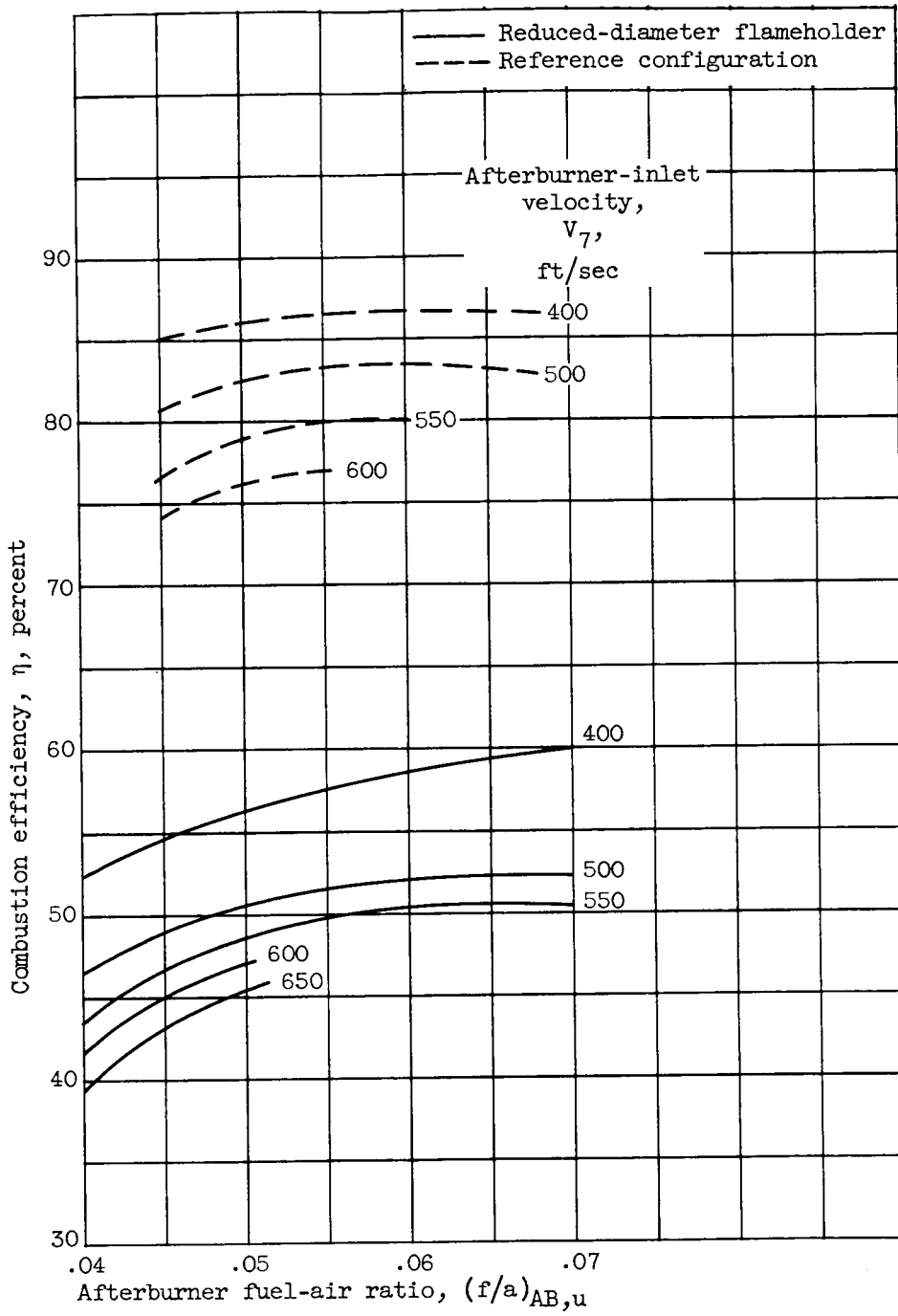

(b) Afterburner-inlet pressure, 1800 pounds per square foot absolute.

Figure 9. - Concluded. Combustion efficiency of reduced-diameter flameholder in $3\frac{1}{2}$-foot afterburner. Afterburner-inlet temperature, 1660° R.

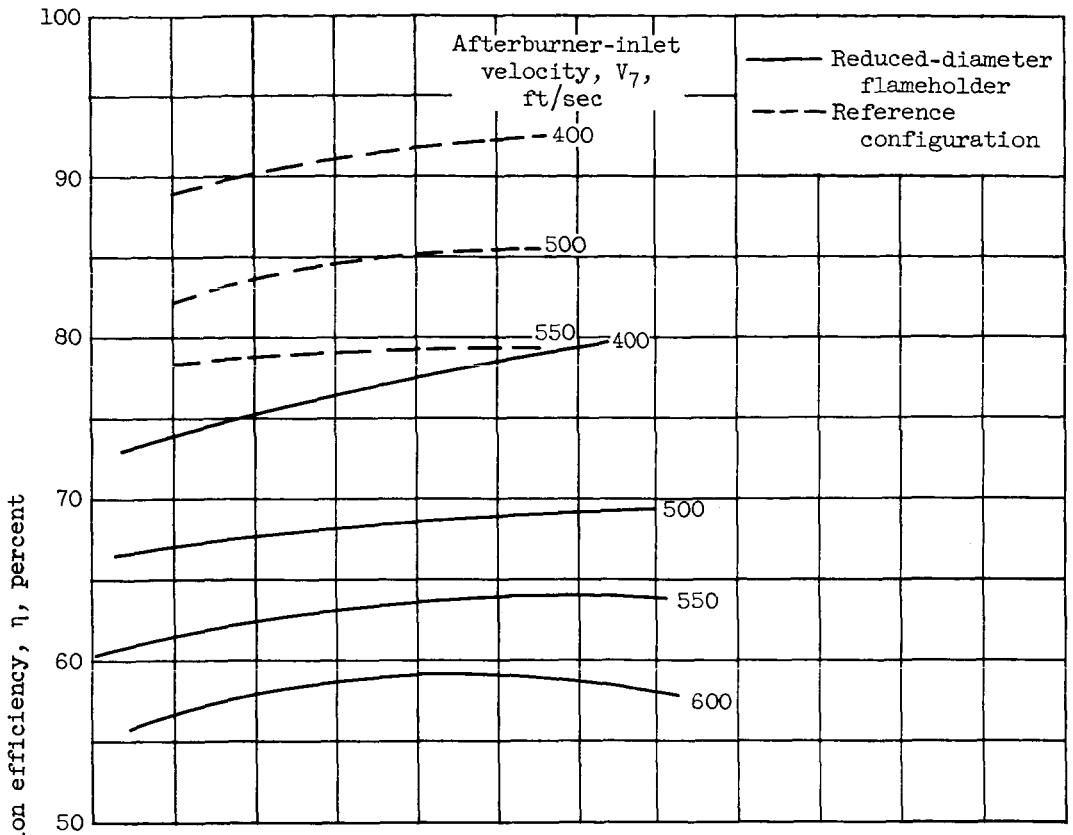

(a) Afterburner-inlet pressure, 750 pounds per square foot absolute.

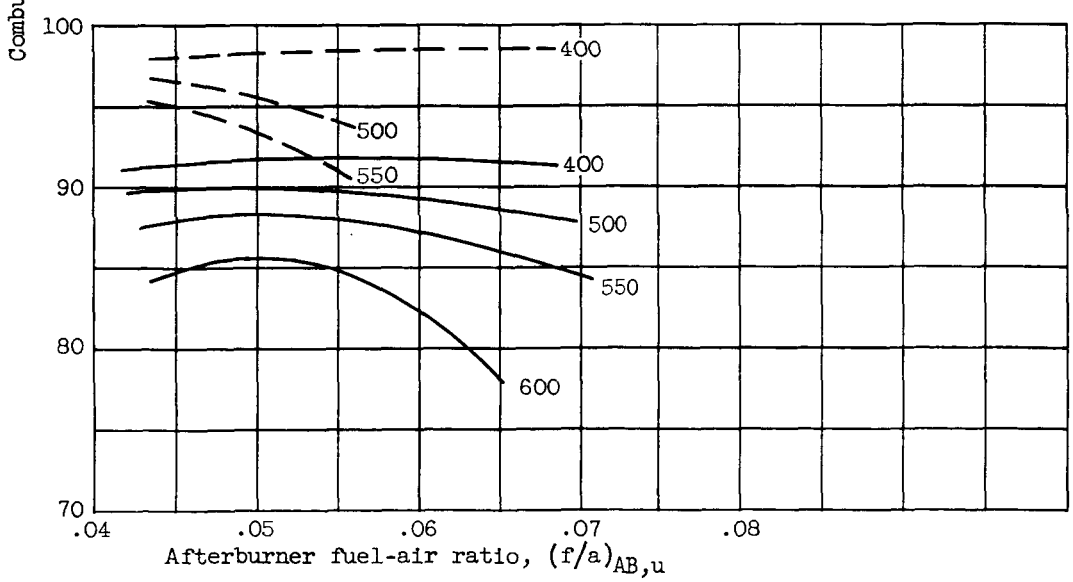

(b) Afterburner-inlet pressure, 1800 pounds per square foot absolute.

Figure 10. - Combustion efficiency of reduced-diameter flameholder in $5\frac{1}{2}$-foot afterburner. Afterburner-inlet temperature, 1660° R.

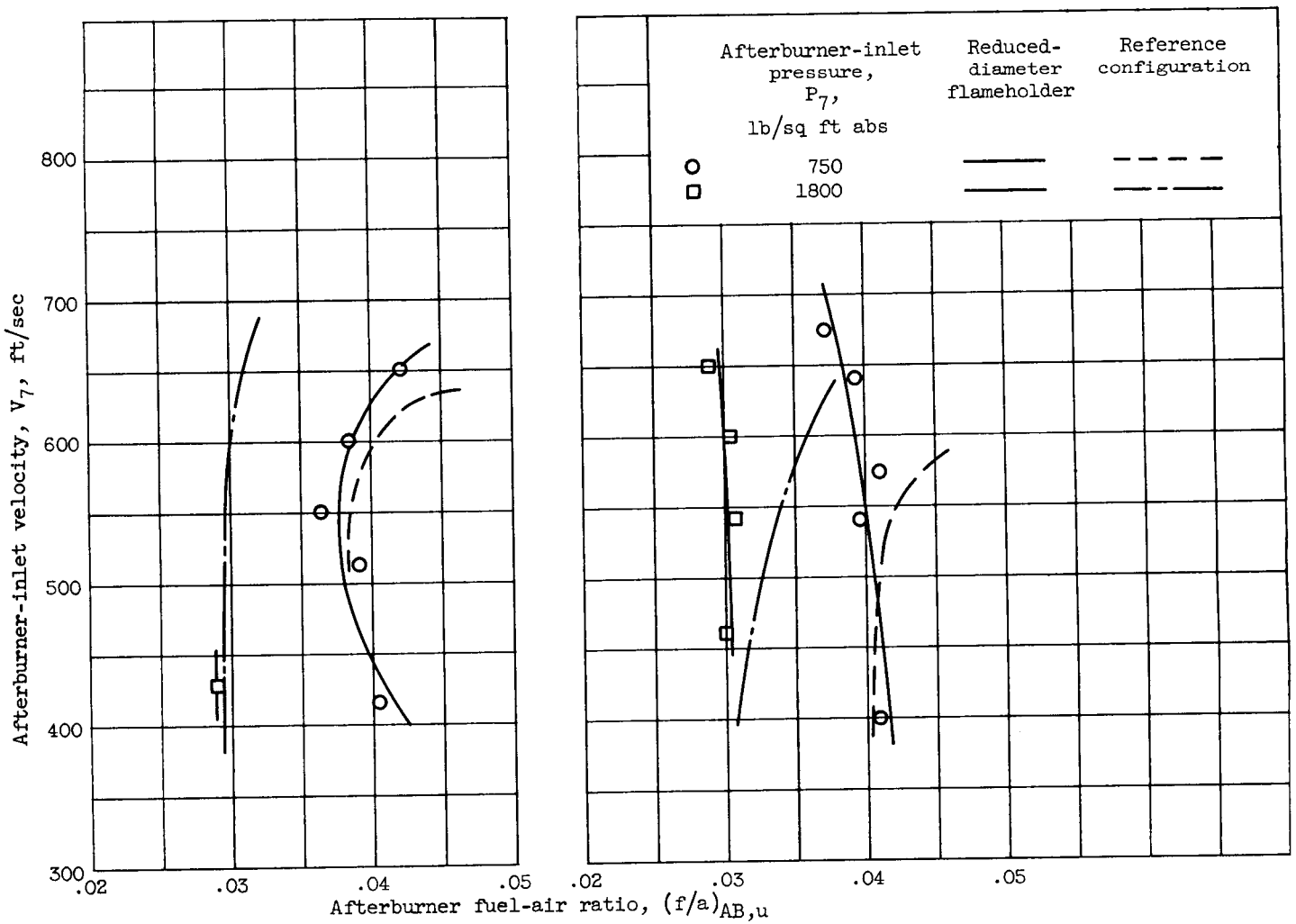

(a) Afterburner length, $3\frac{1}{2}$ feet.

(b) Afterburner length, $5\frac{1}{2}$ feet.

Figure 11. - Lean blowout limits of reduced-diameter flameholder. Afterburner-inlet temperature, 1660° R.

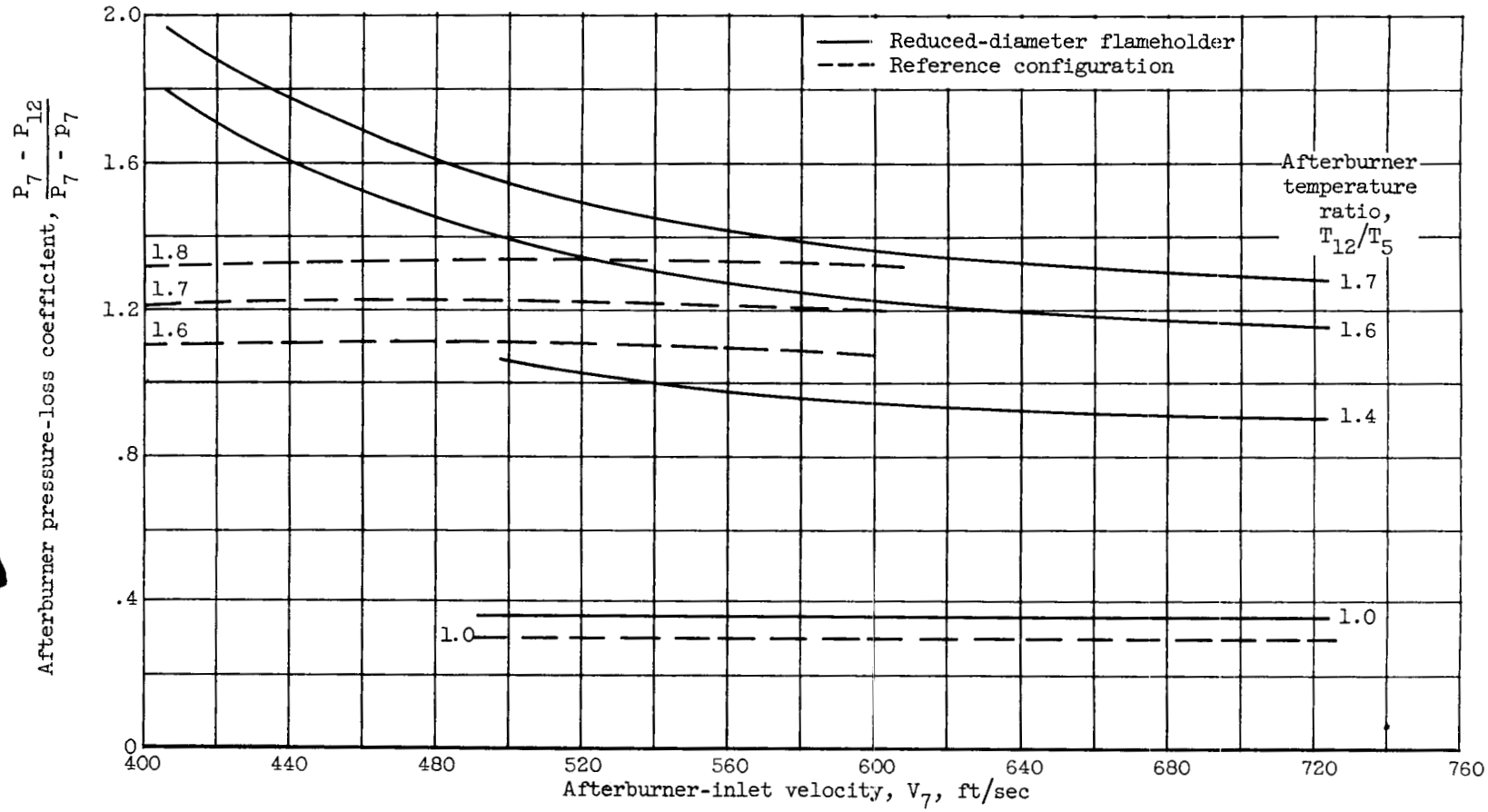

(a) Afterburner length, $3\frac{1}{2}$ feet.

Figure 12. - Afterburner pressure-loss coefficient with reduced-diameter flameholder. Afterburner-inlet temperature, 1660° R; afterburner-inlet pressure, 750 pounds per square inch absolute.

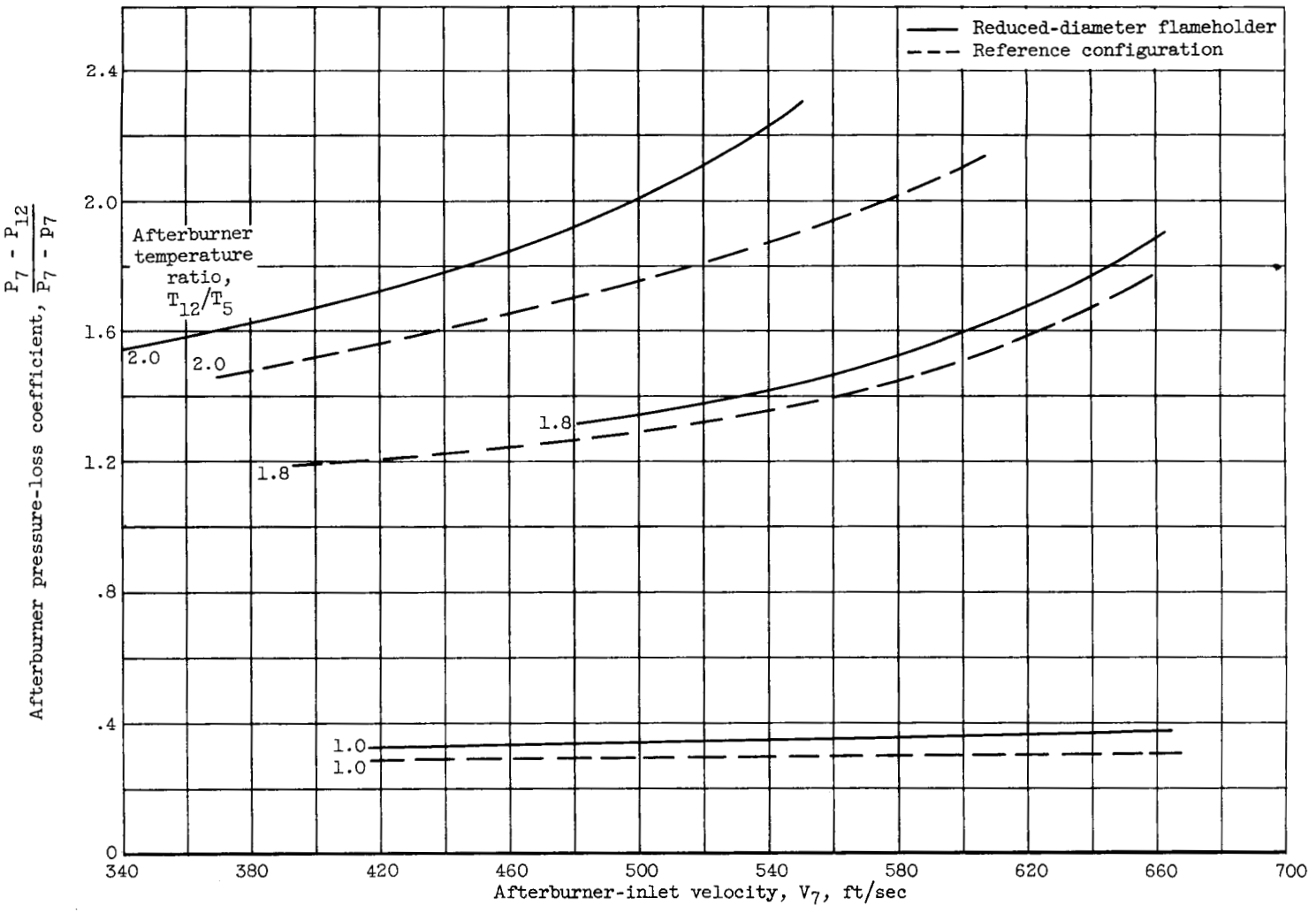

(b) Afterburner length, $5\frac{1}{2}$ feet.

Figure 12. - Concluded. Afterburner pressure-loss coefficient with reduced-diameter flameholder. Afterburner-inlet temperature, 1660° R; afterburner-inlet pressure, 750 pounds per square inch absolute.

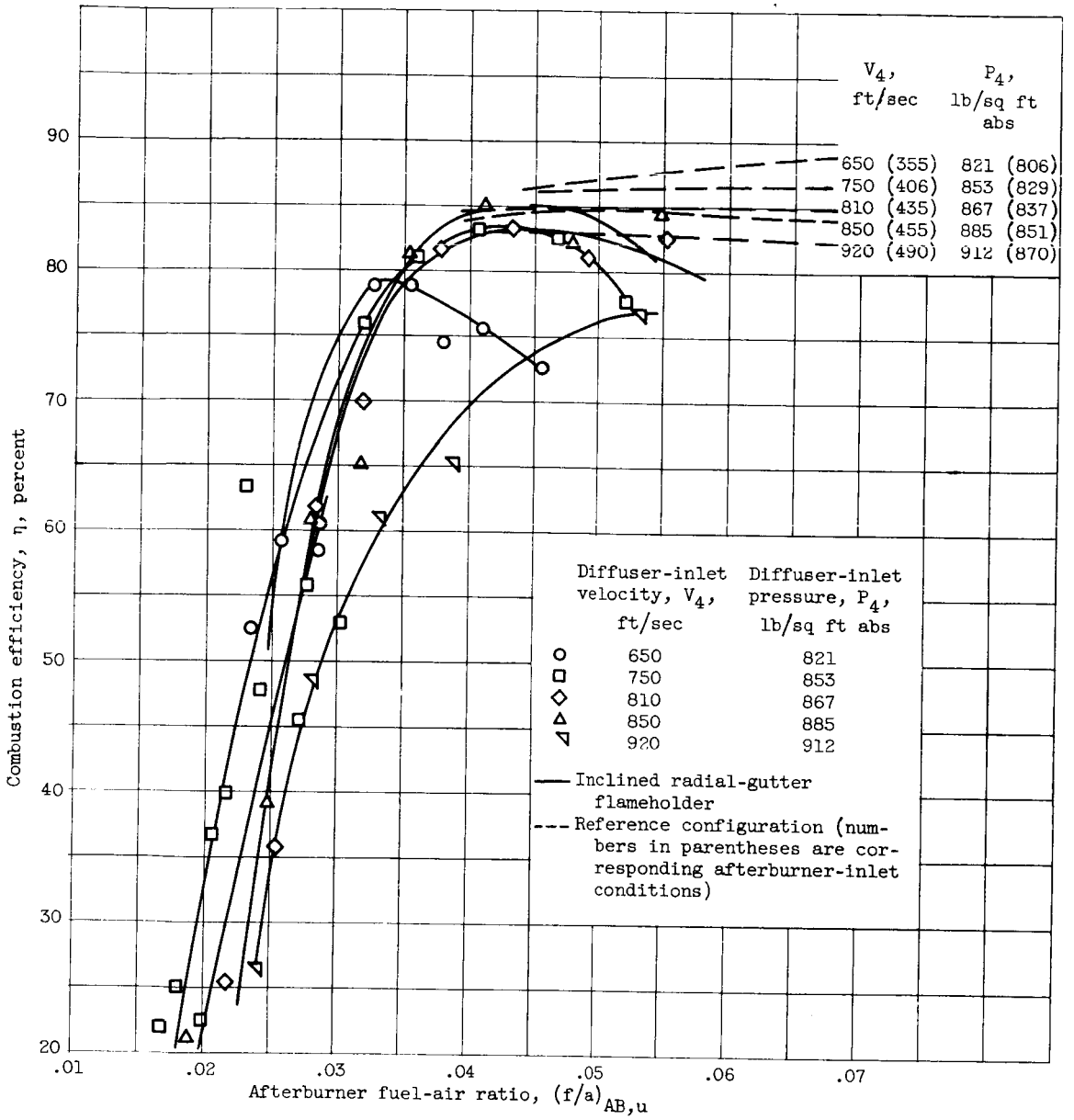

(a) Low-pressure conditions.

Figure 13. - Combustion efficiency of inclined radial-gutter flameholder with short cooling liner. Afterburner-inlet temperature, 1660° R; afterburner length, $4\frac{1}{2}$ feet.

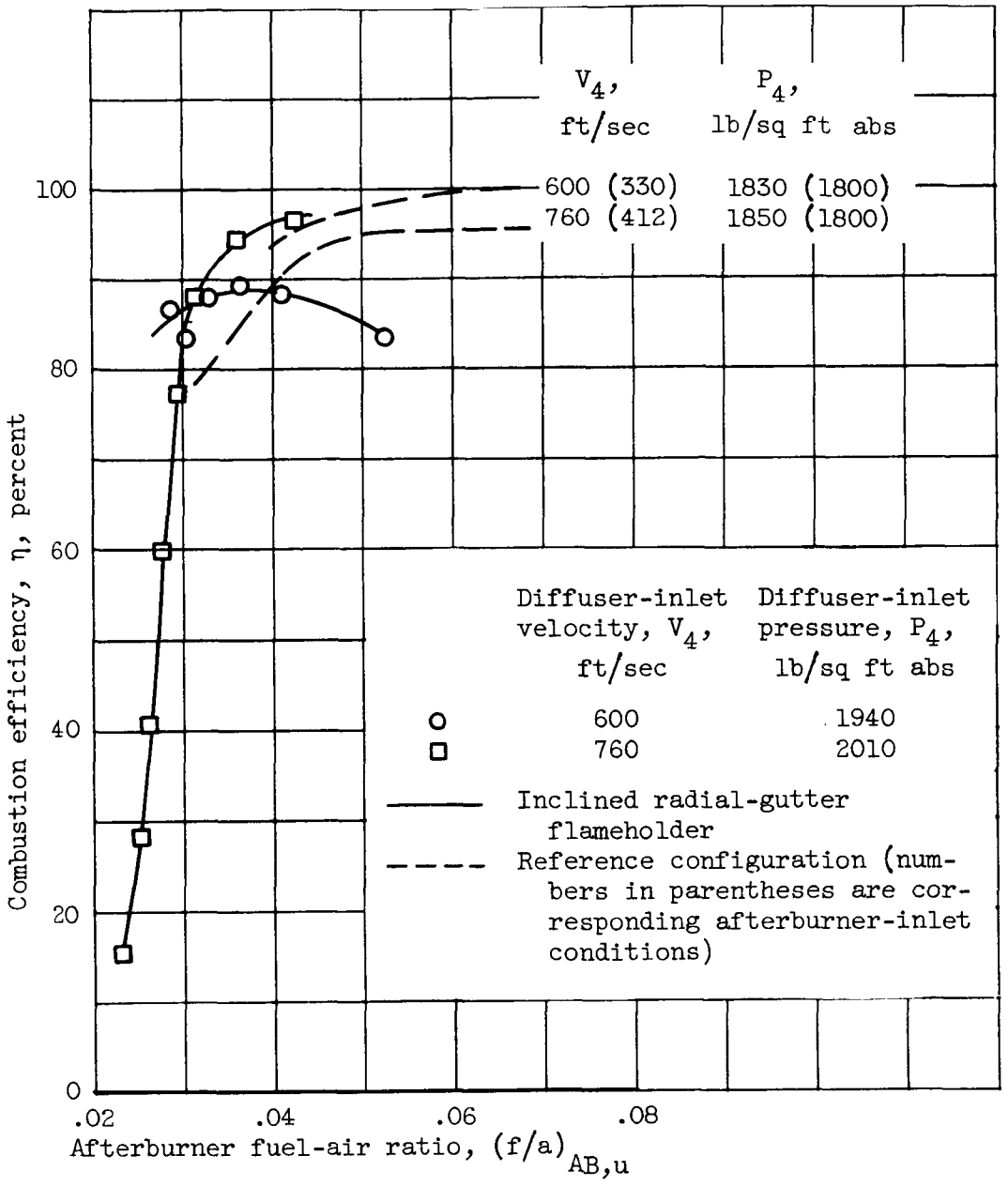

(b) High-pressure conditions.

Figure 13. - Concluded. Combustion efficiency of inclined radial-gutter flameholder with short cooling liner. Afterburner-inlet temperature, 1660° R; afterburner length, $4\frac{1}{2}$ feet.

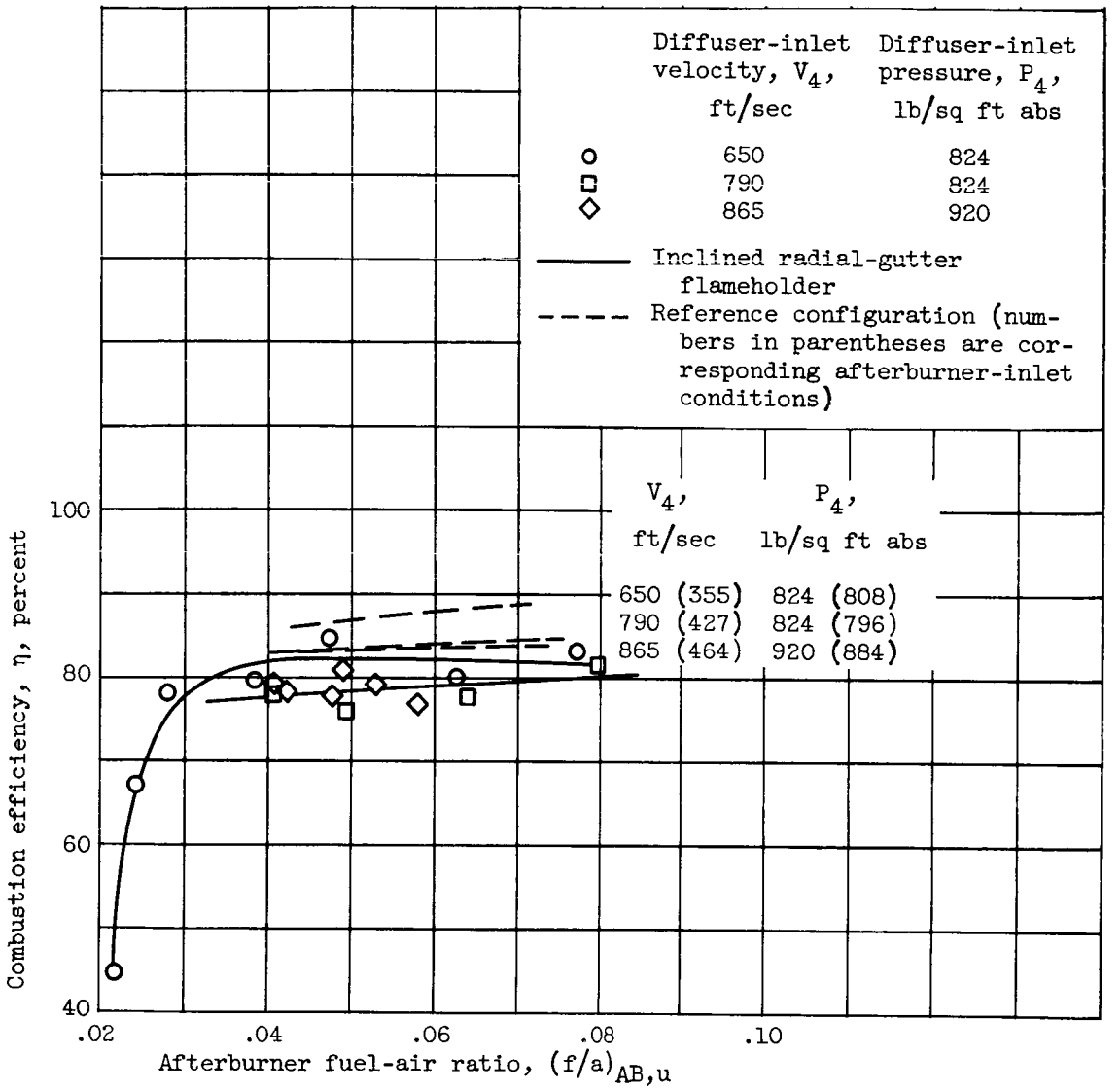

(a) Low-pressure conditions.

Figure 14. - Combustion efficiency of inclined radial-gutter flameholder with long cooling liner. Afterburner-inlet temperature, 1660° R; afterburner length, $4\frac{1}{2}$ feet.

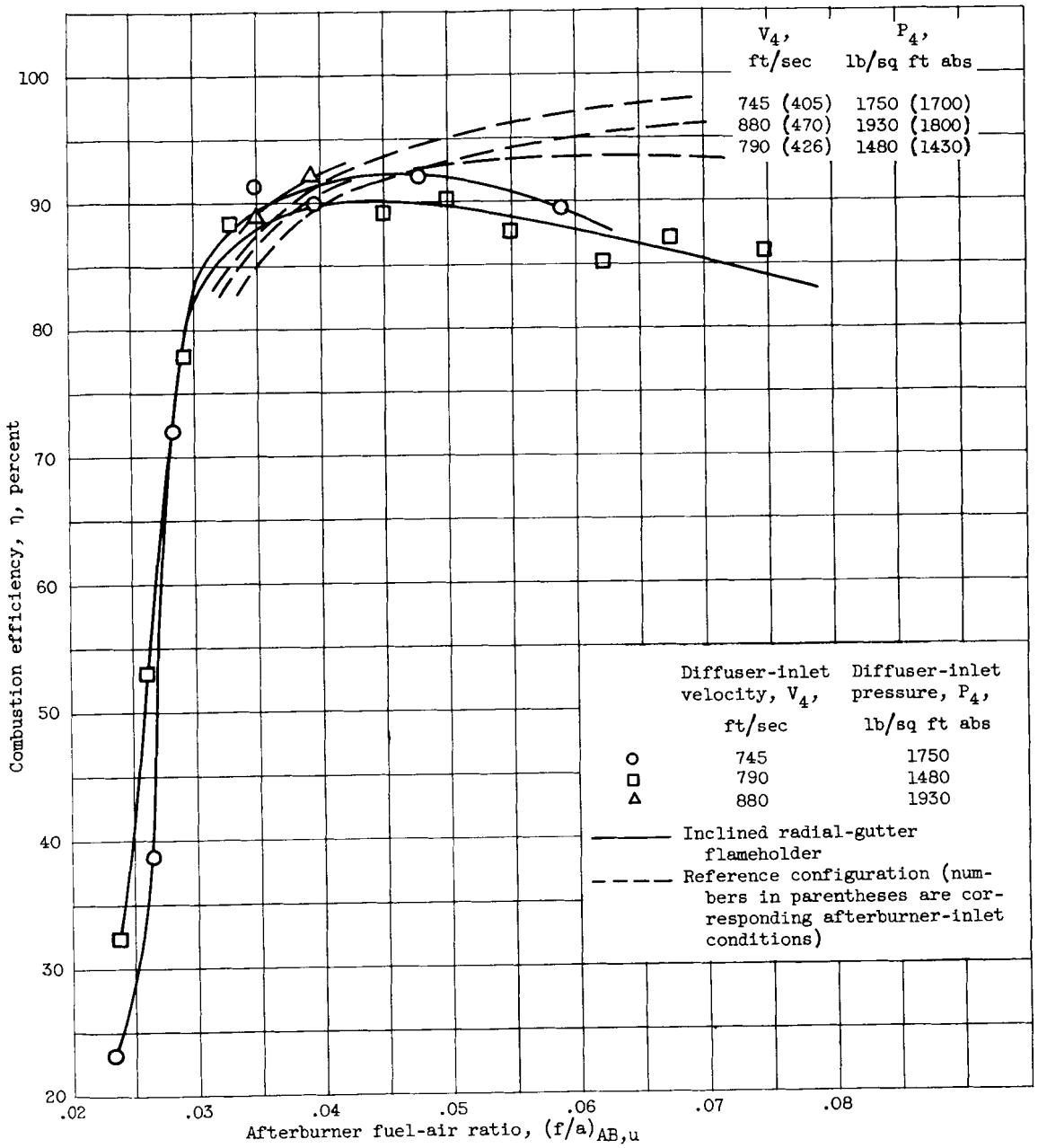

(b) High-pressure conditions.

Figure 14. - Concluded. Combustion efficiency of inclined radial-gutter flameholder with long cooling liner. Afterburner-inlet temperature, 1660° R; afterburner length, $4\frac{1}{2}$ feet.

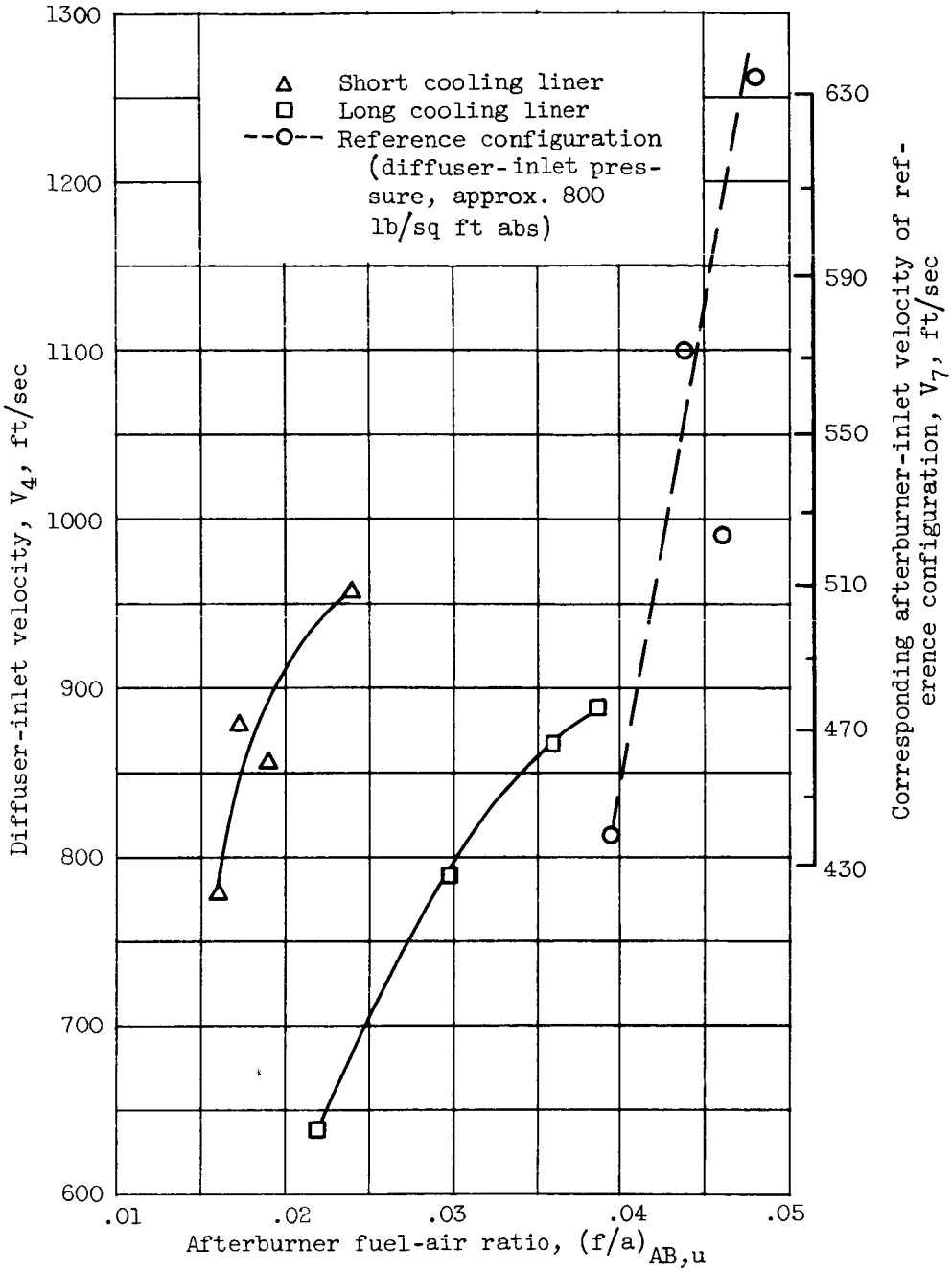

(a) Low diffuser-inlet pressure.

Figure 15. - Lean blowout limits of inclined radial-gutter flameholder with long and short cooling liners. Afterburner-inlet temperature, 1660° R; afterburner length, $4\frac{1}{2}$ feet.

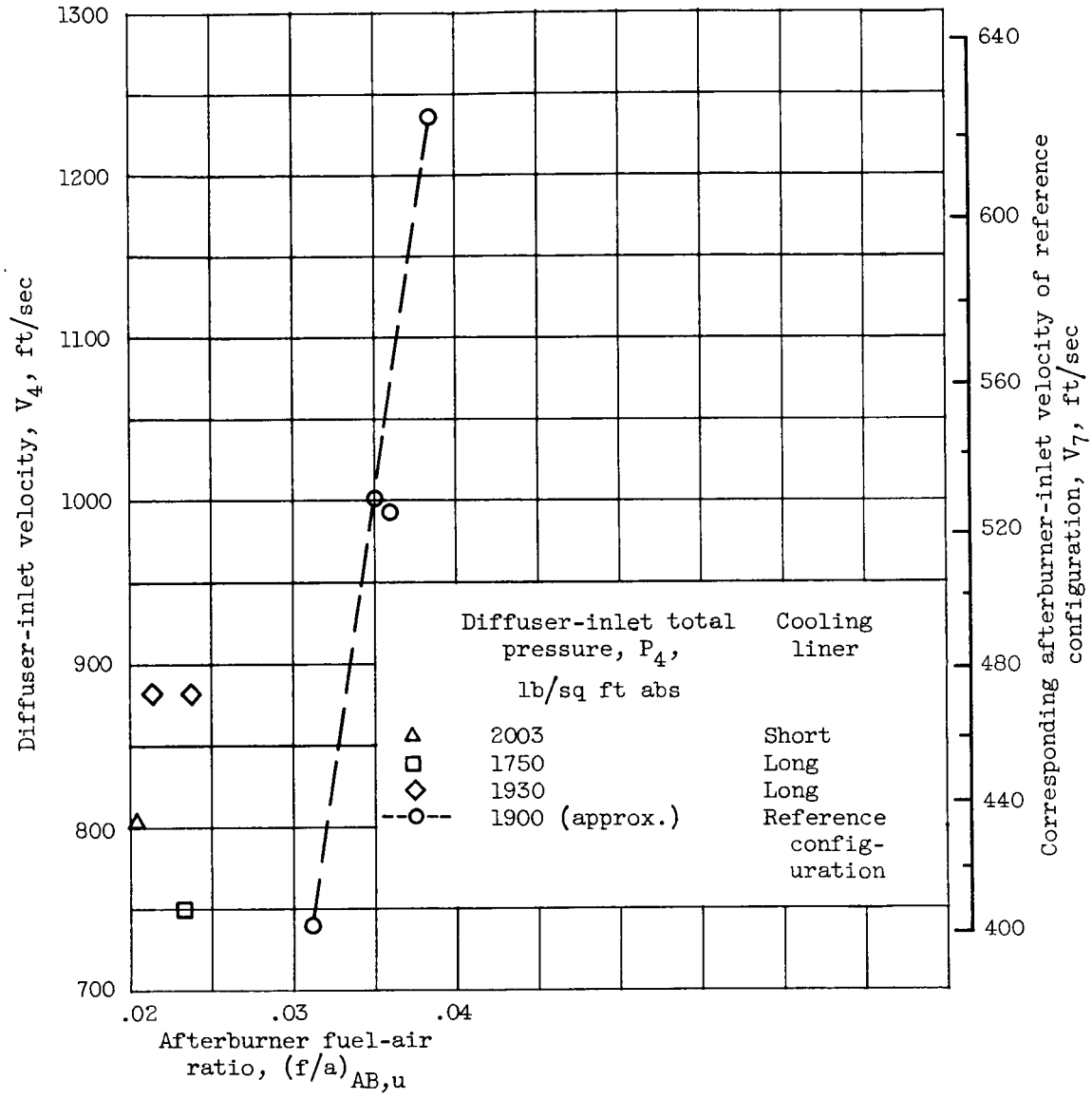

(b) High diffuser-inlet pressure.

Figure 15. - Concluded. Lean blowout limits of inclined radial-gutter flameholder with long and short cooling liners. Afterburner-inlet temperature, 1660° R; afterburner length, $4\frac{1}{2}$ feet.

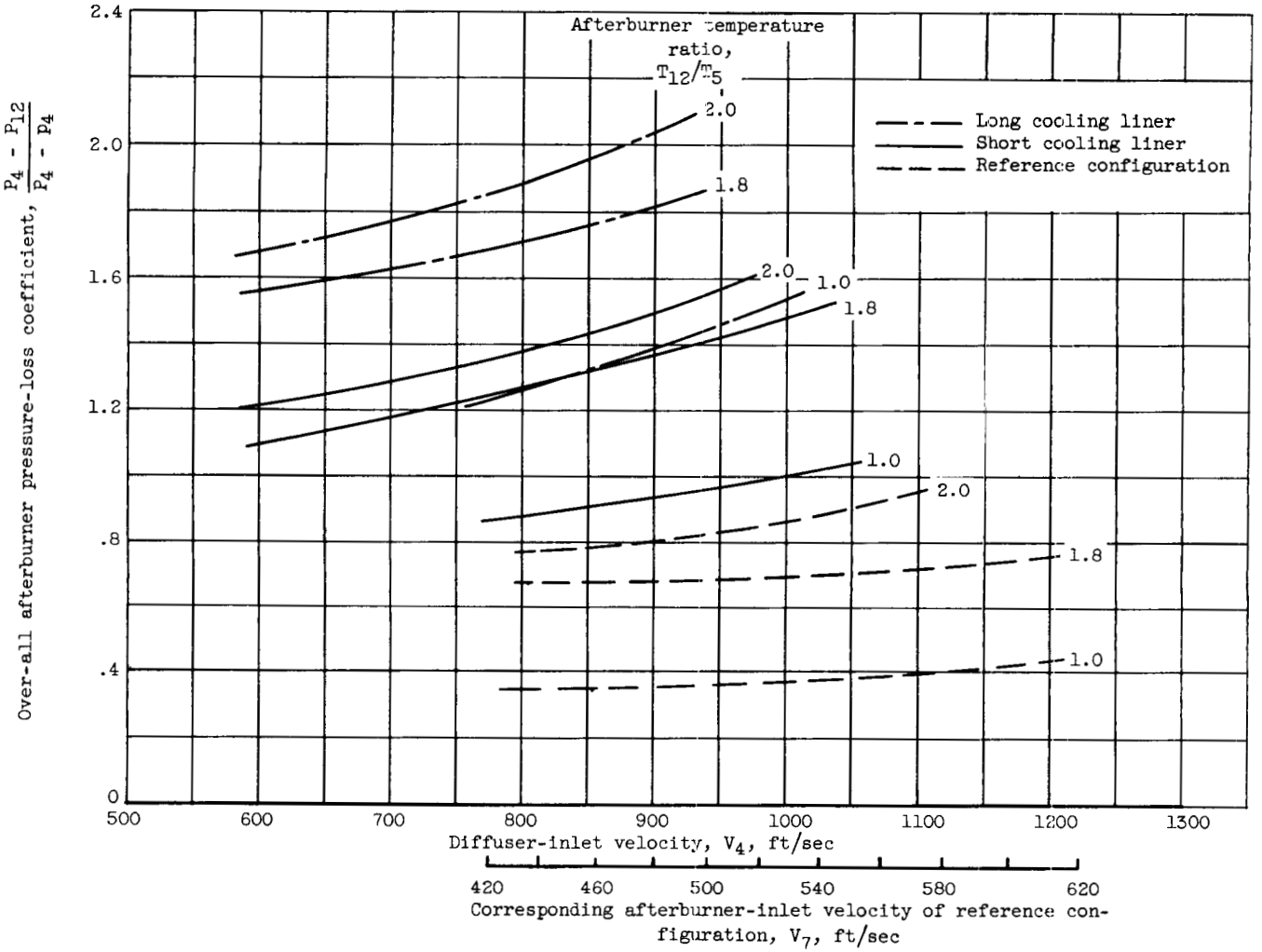

Figure 16. - Over-all afterburner pressure-loss coefficient of inclined radial-gutter flameholder with long and short cooling liners. Afterburner-inlet temperature, 1660° R; diffuser-inlet pressures, 820 to 2000 pounds per square foot absolute (approx. afterburner-inlet pressures, 780 to 1900 lb/sq ft); afterburner length, $4\frac{1}{2}$ feet.

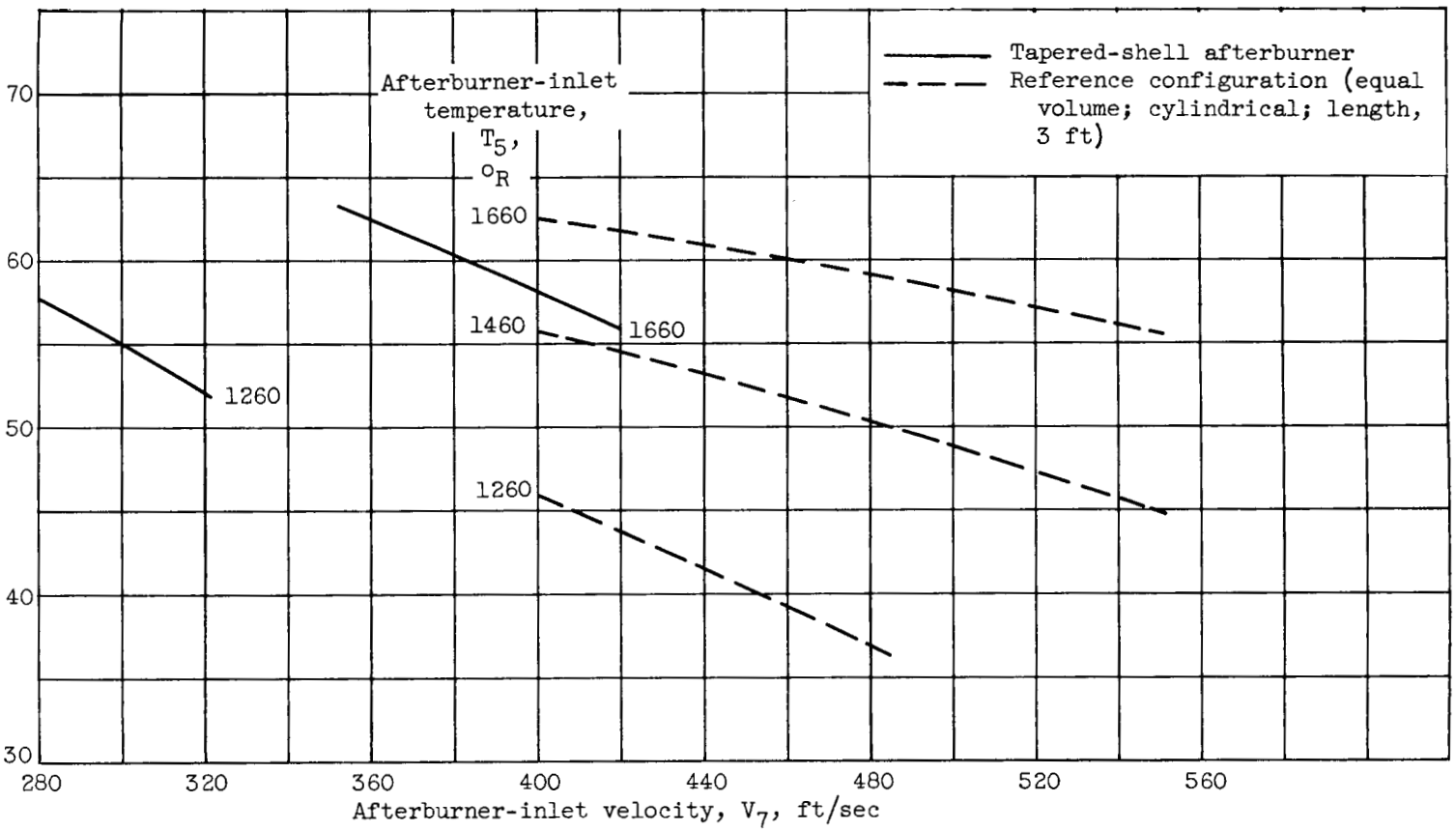

(a) Afterburner-inlet pressure, 750 pounds per square foot absolute.

Figure 17. - Comparative combustion efficiencies of tapered-shell afterburner at afterburner fuel-air ratio of 0.055. Shell taper, 5° half-angle; afterburner length, $3\frac{1}{2}$ feet.

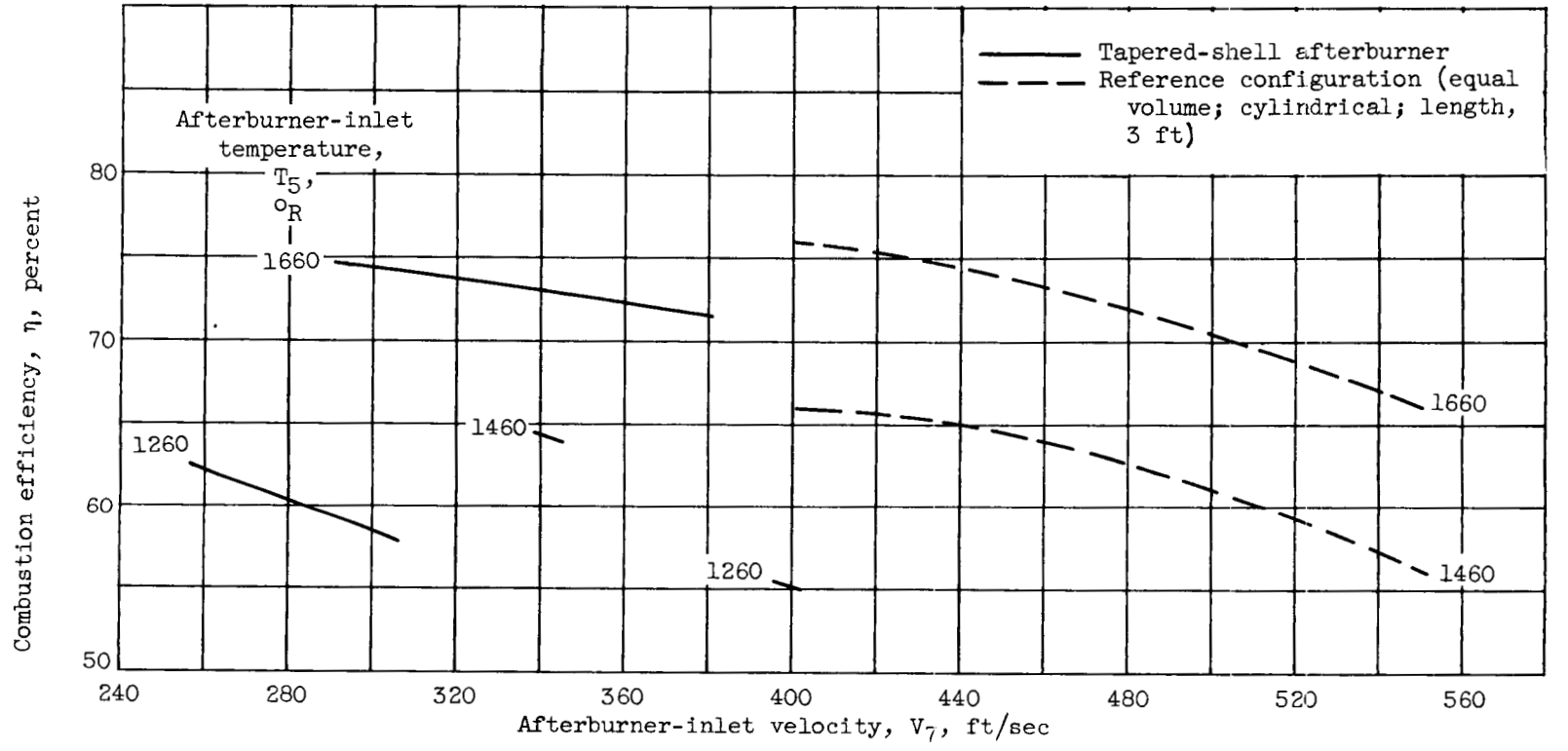

(b) Afterburner-inlet pressure, 1270 pounds per square foot absolute.

Figure 17. - Continued. Comparative combustion efficiencies of tapered-shell afterburner at afterburner fuel-air ratio of 0.055. Shell taper, 5° half-angle; afterburner length, $3\frac{1}{2}$ feet.

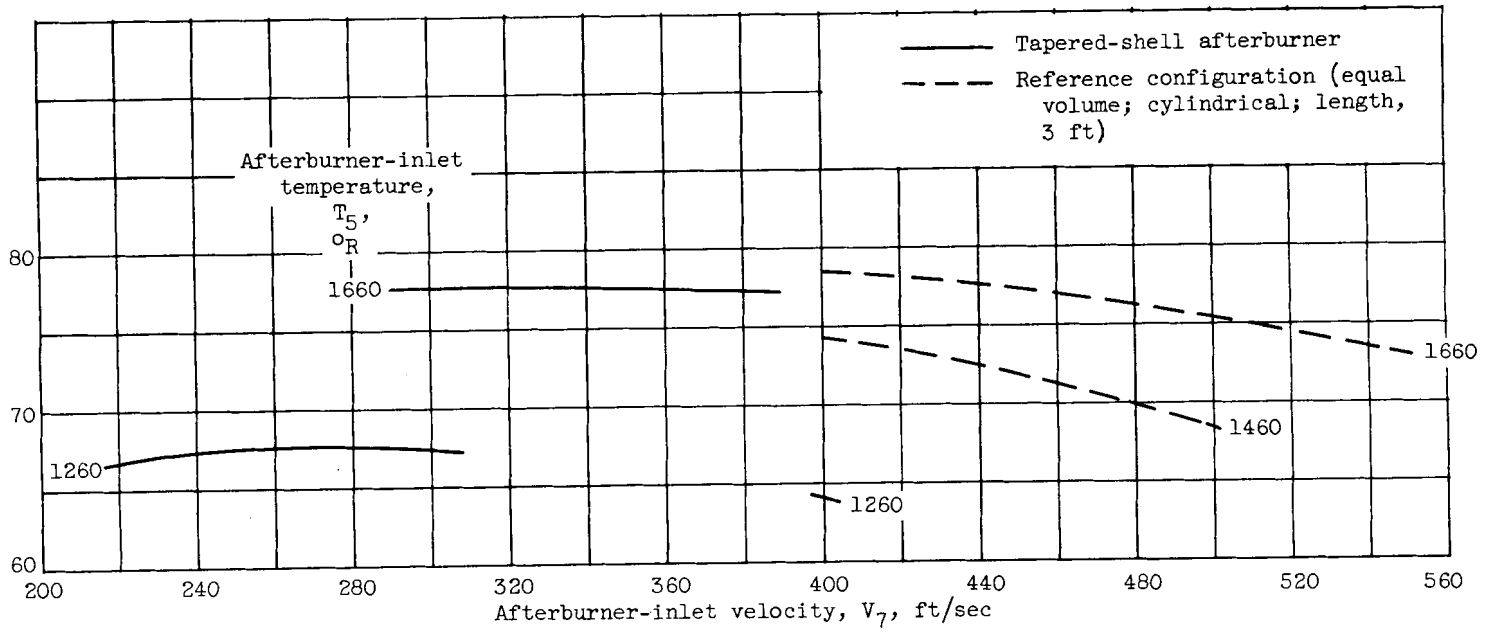

(c) Afterburner-inlet pressure, 1800 pounds per square foot absolute.

Figure 17. - Concluded. Comparative combustion efficiencies of tapered-shell afterburner at afterburner fuel-air ratio of 0.055. Shell taper, 5° half-angle; afterburner length, $3\frac{1}{2}$ feet.

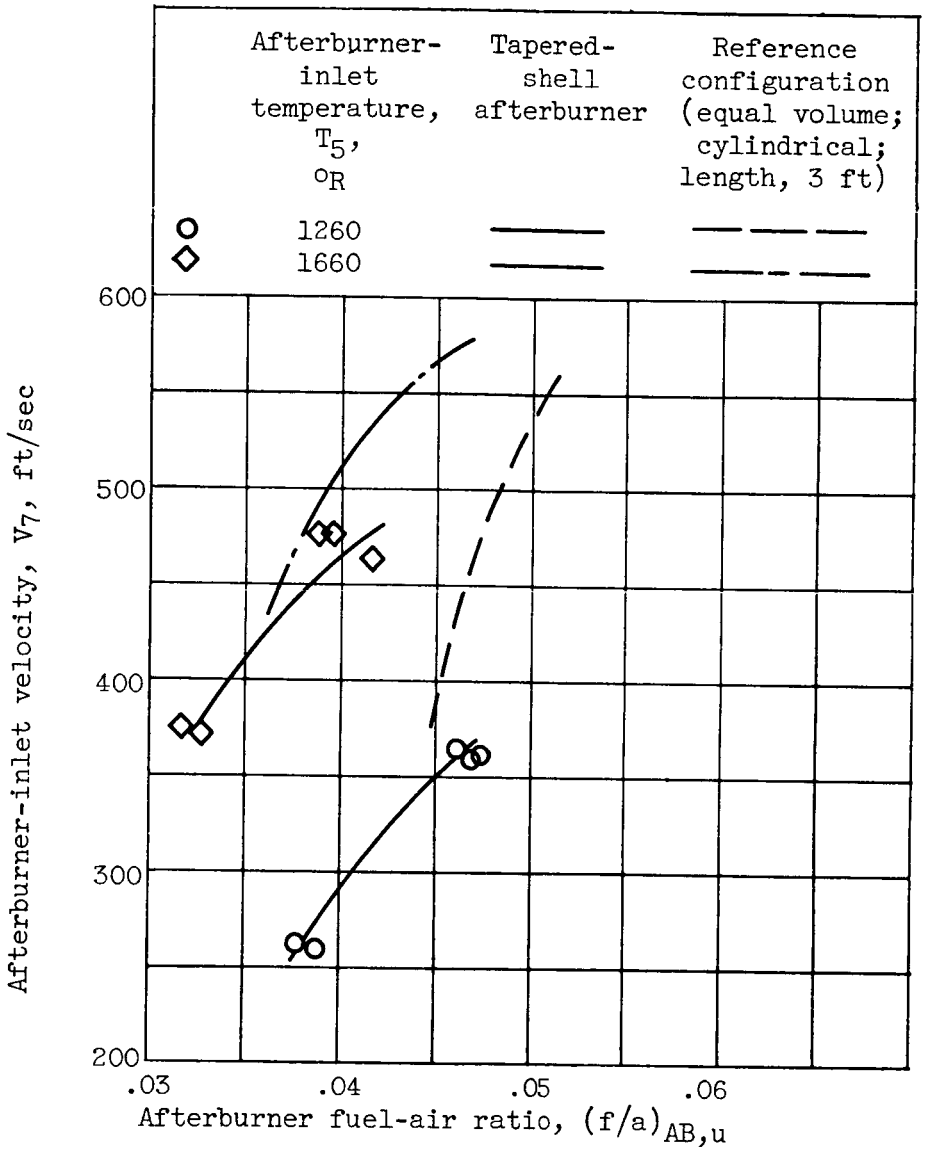

(a) Afterburner-inlet pressure, 750 pounds per square foot absolute.

Figure 18. - Lean blowout limits of tapered-shell afterburner. Shell taper, 5° half-angle; afterburner length, $3\frac{1}{2}$ feet.

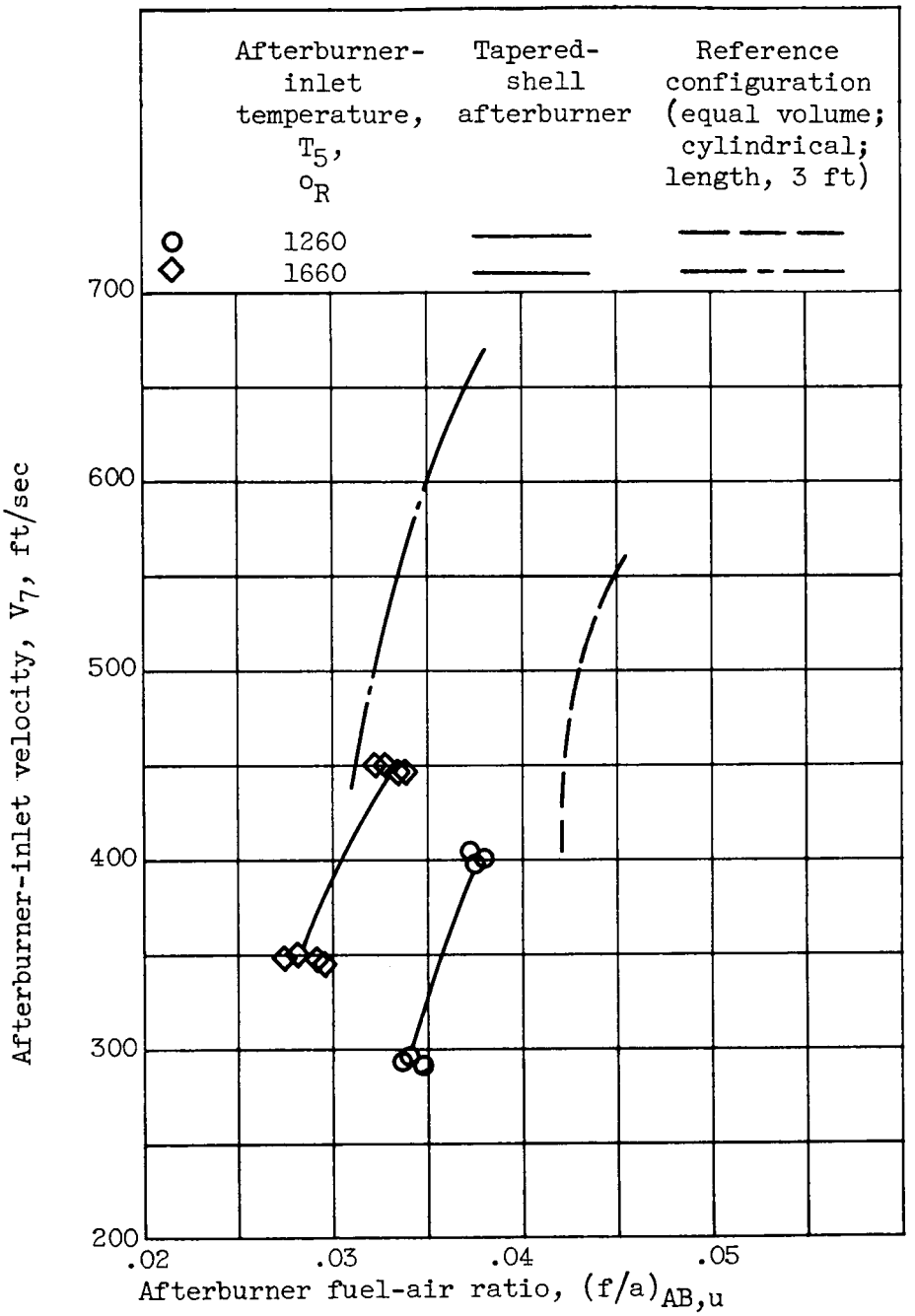

(b) Afterburner-inlet pressure, 1270 pounds per square foot absolute.

Figure 18. - Continued. Lean blowout limits of tapered-shell afterburner. Shell taper, 5° half-angle; afterburner length, $3\frac{1}{2}$ feet.

[redacted]

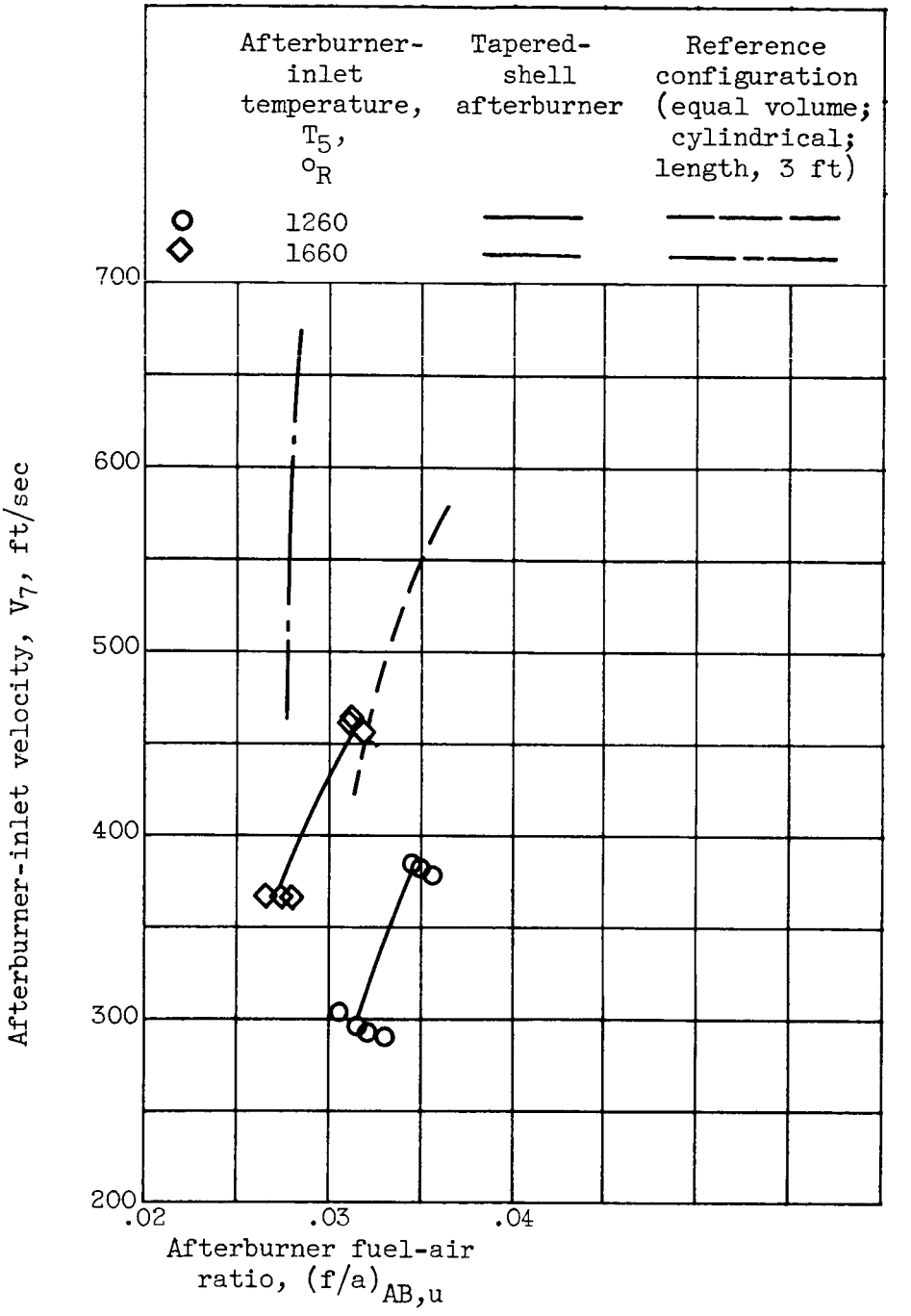

(c) Afterburner-inlet pressure, 1800 pounds per square foot absolute.

Figure 18. - Concluded. Lean blowout limits of tapered-shell afterburner. Shell taper, 5° half-angle; afterburner length, $3\frac{1}{2}$ feet.

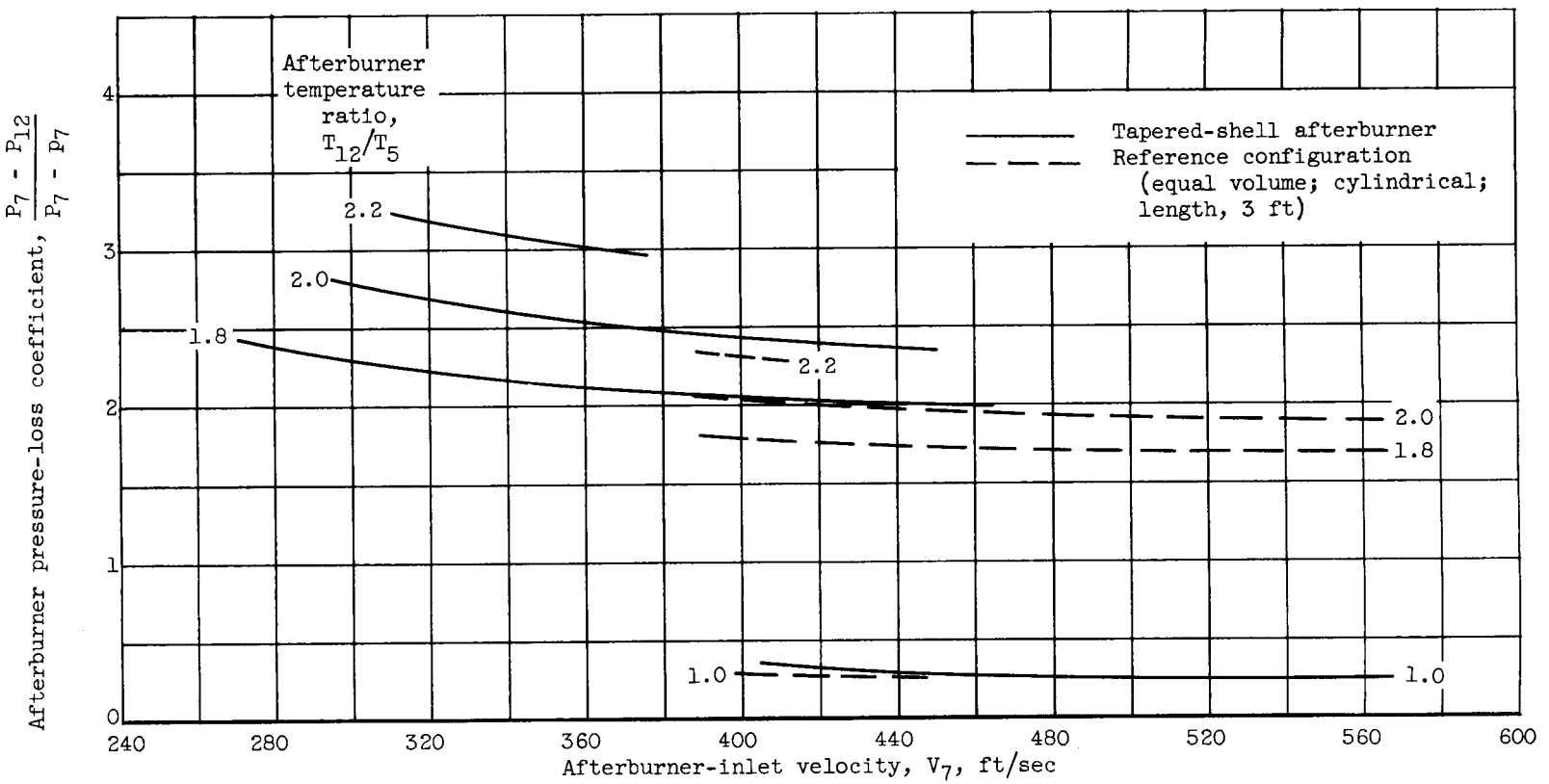

Figure 19. - Afterburner pressure-loss coefficient of tapered-shell afterburner. Shell taper, 5° half-angle; afterburner length, $3\frac{1}{2}$ feet; afterburner-inlet pressures, 750 to 1800 pounds per square foot absolute.

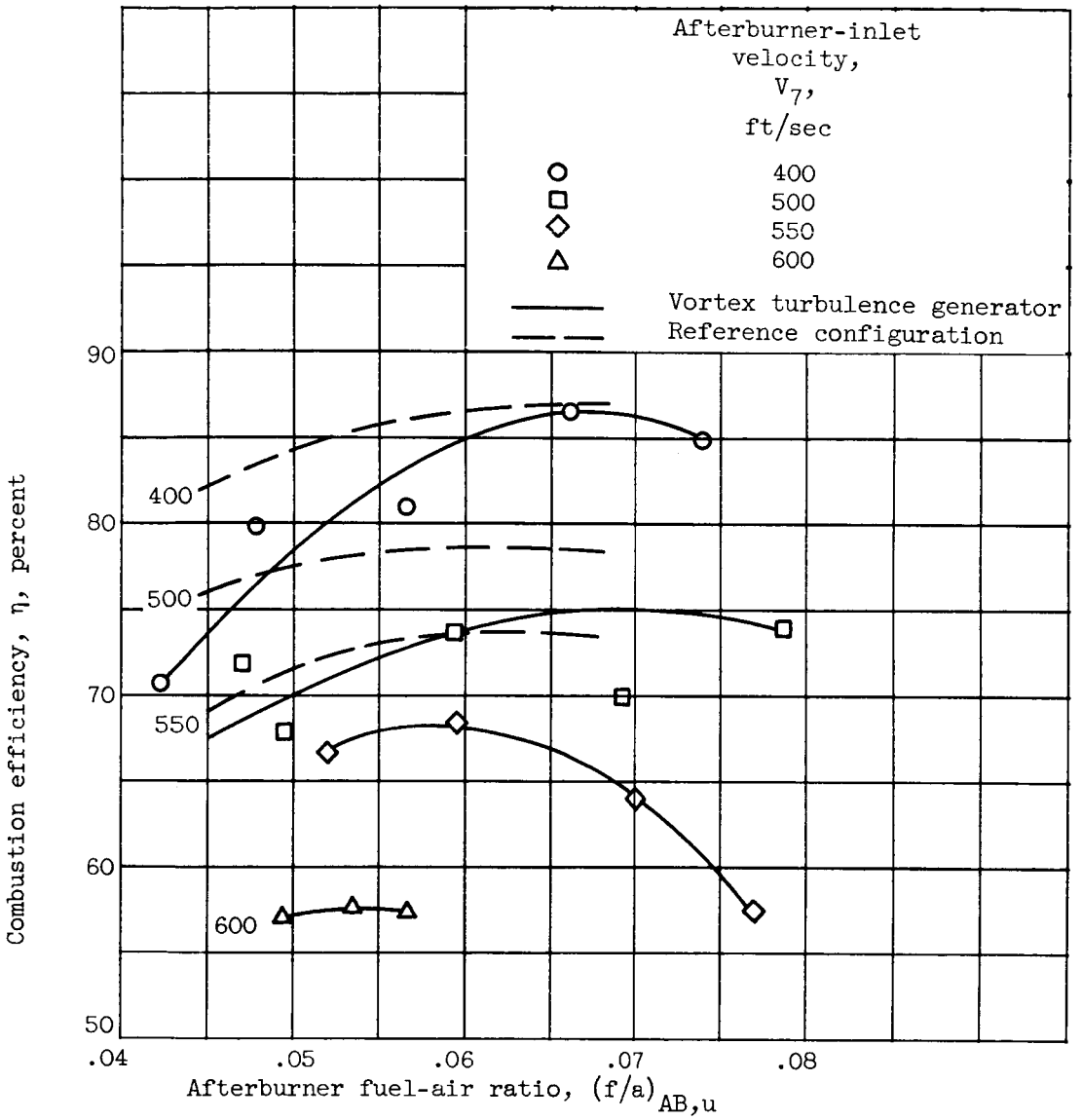

Figure 20. - Combustion efficiency of vortex turbulence generator. Afterburner-inlet temperature, 1660° R; afterburner-inlet pressure, 750 pounds per square foot absolute; afterburner length, $4\frac{1}{2}$ feet.

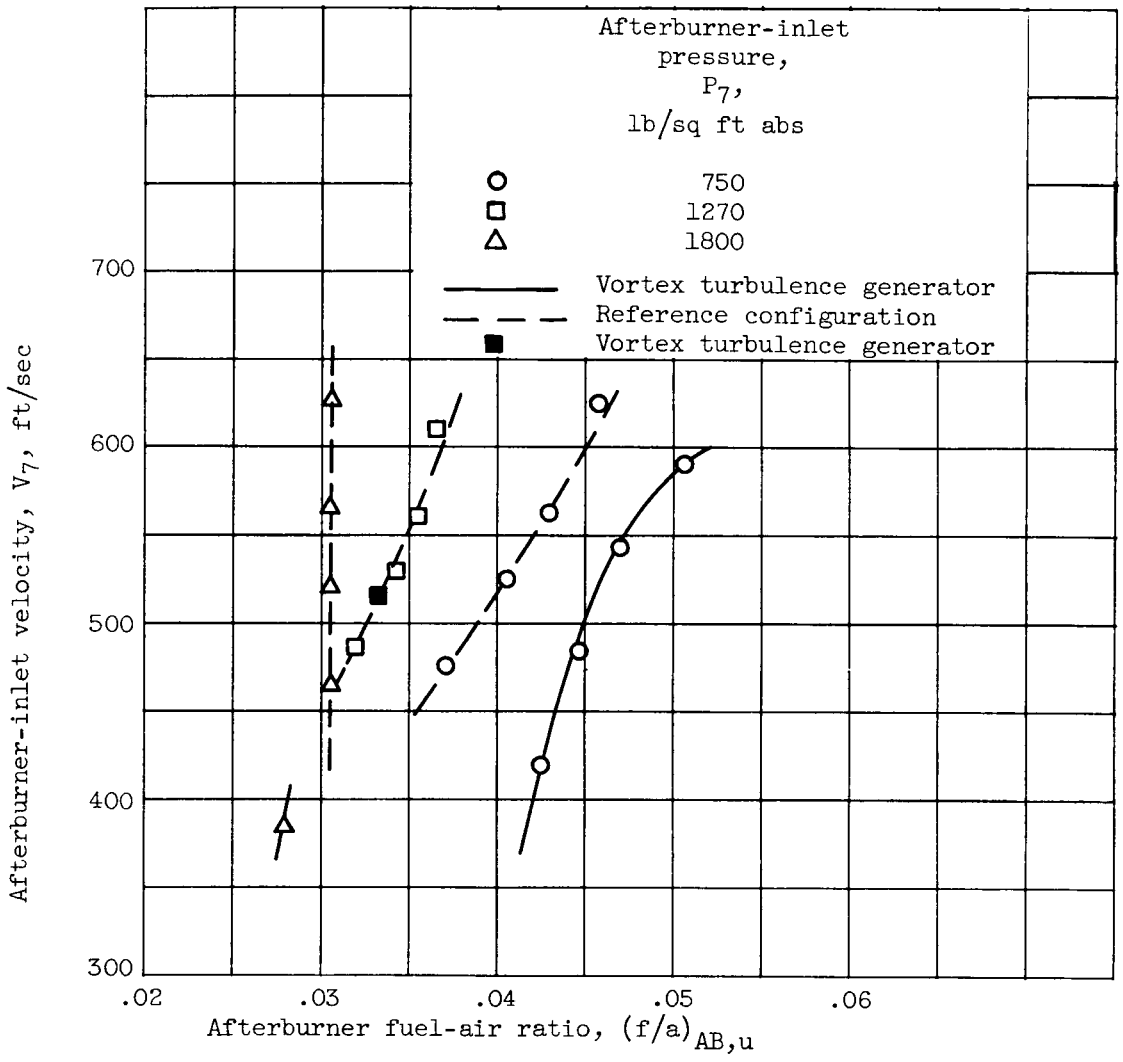

Figure 21. - Lean blowout limits of vortex turbulence generator. Afterburner-inlet temperature, 1660° R; afterburner length, $4\frac{1}{2}$ feet.

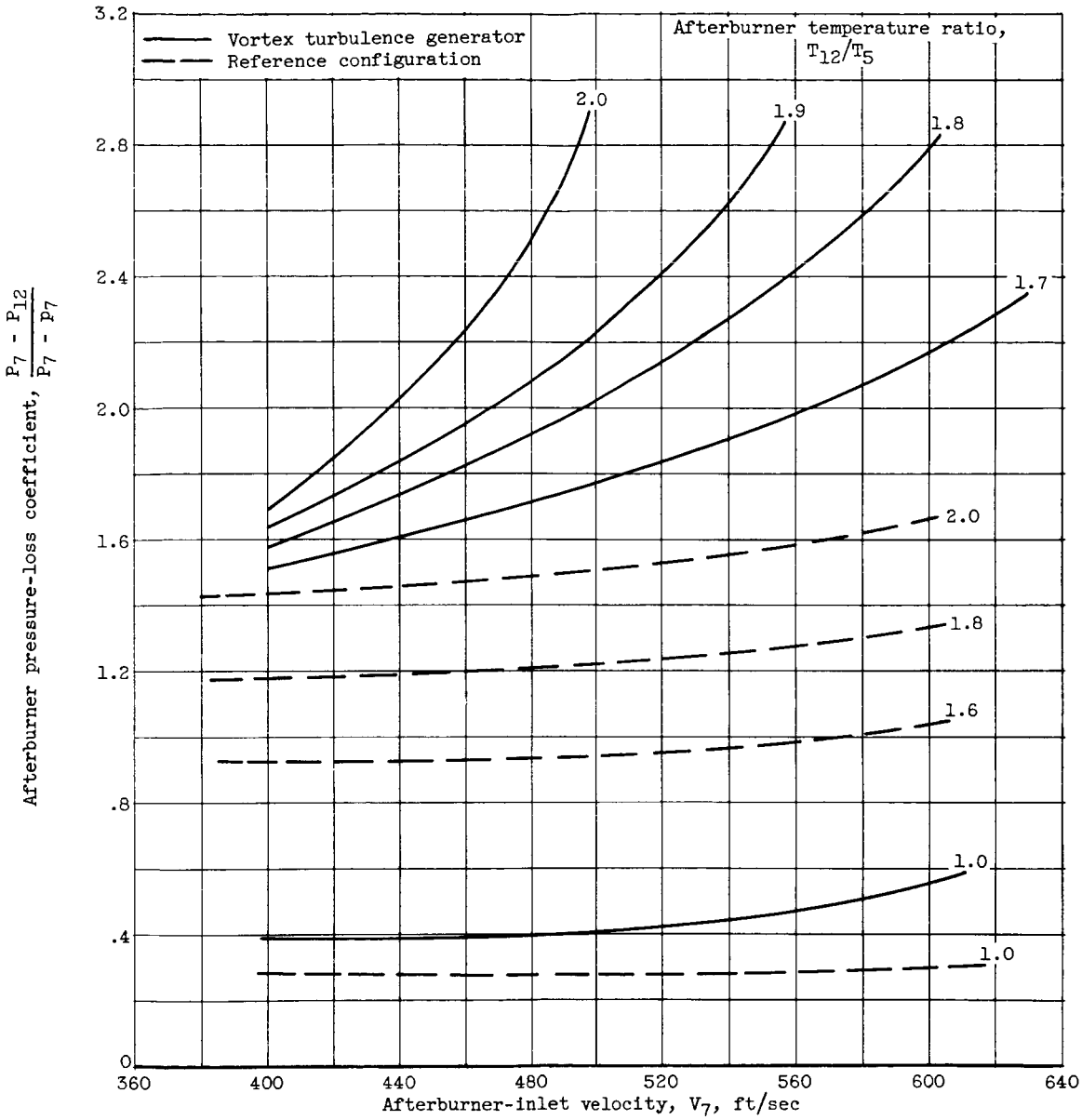

Figure 22. - Afterburner pressure-loss coefficient of vortex turbulence generator. Afterburner-inlet temperature, 1660° R; afterburner-inlet pressure, 750 pounds per square foot absolute; afterburner length, $4\frac{1}{2}$ feet.

[redacted]

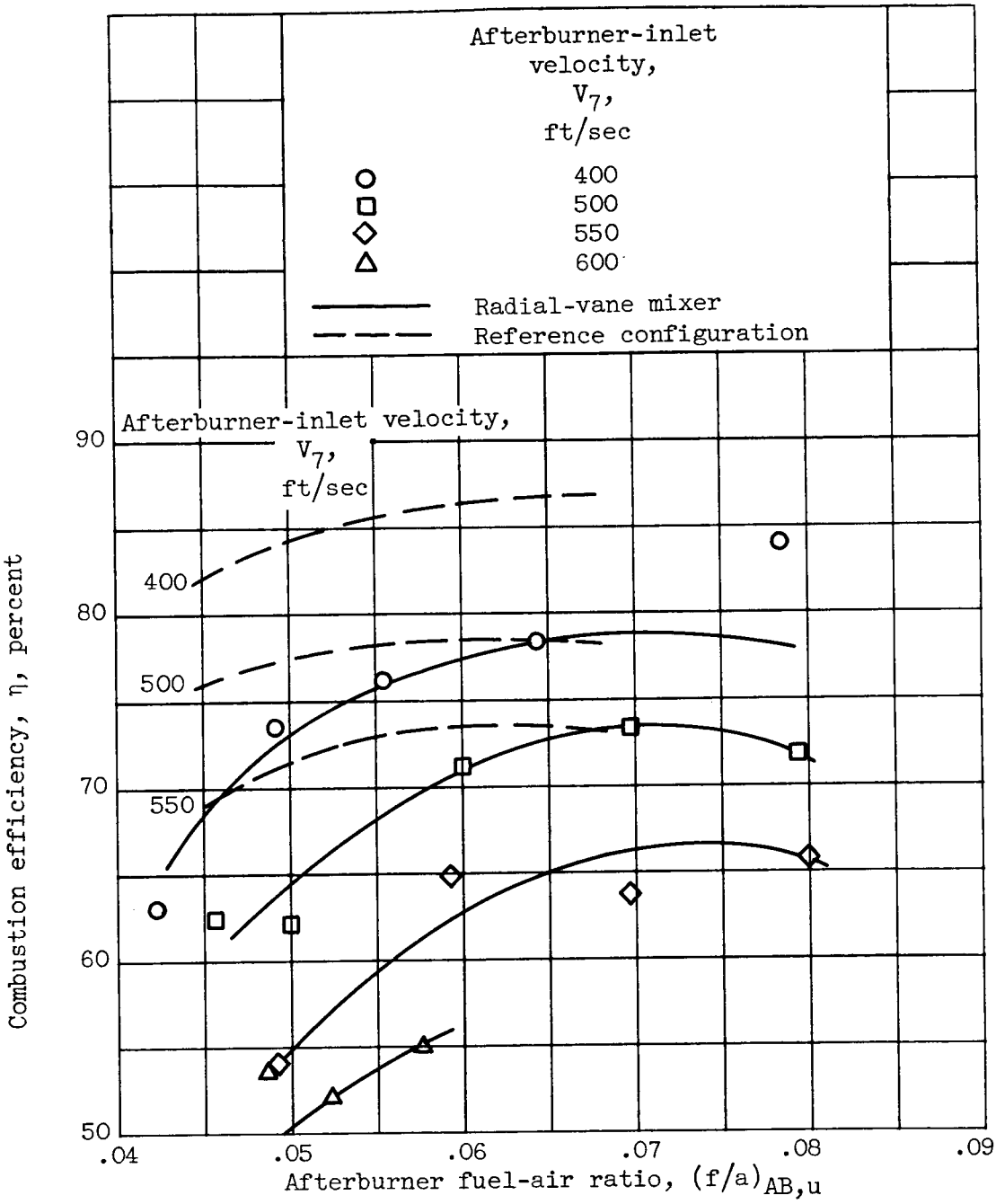

Figure 23. - Combustion efficiency of radial-vane mixer. Afterburner-inlet temperature, 1660° R; afterburner-inlet pressure, 750 pounds per square foot absolute; afterburner length, $4\frac{1}{2}$ feet.

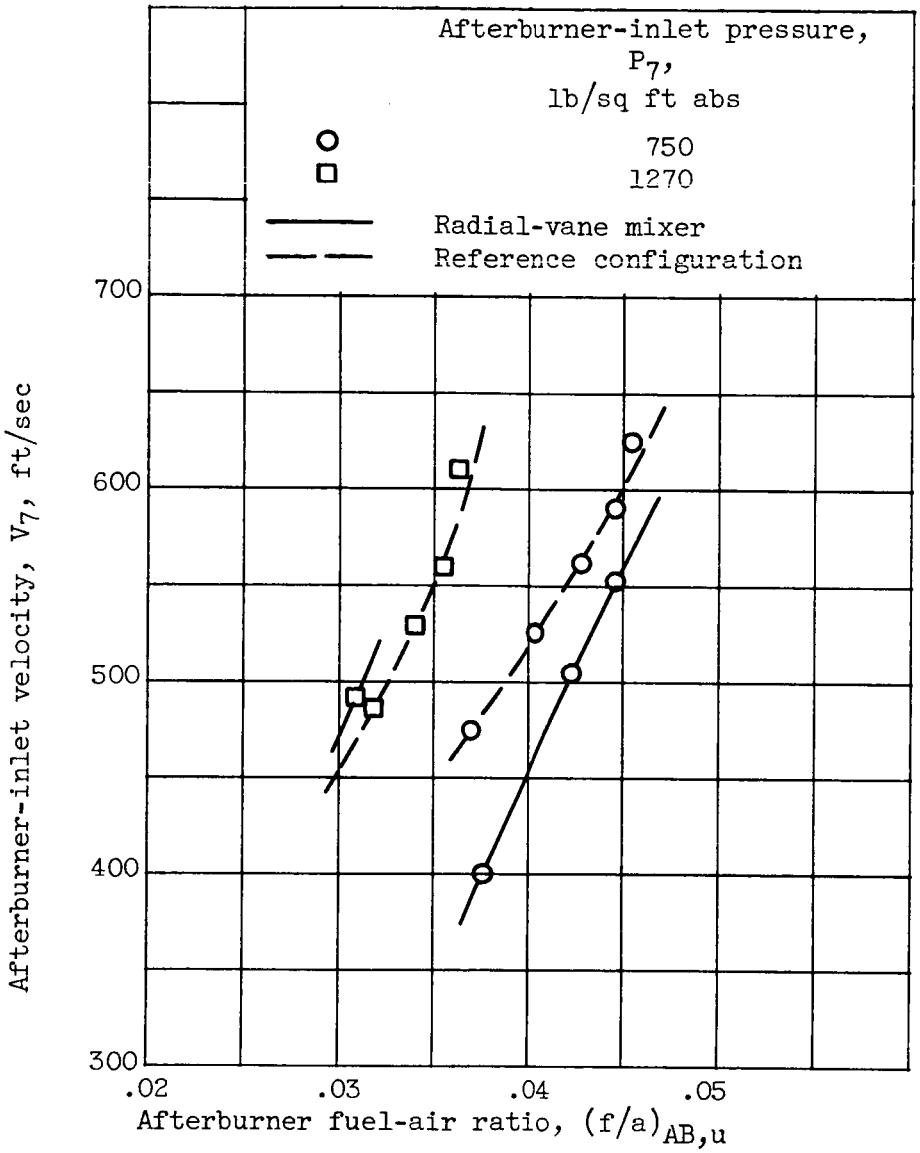

Figure 24. - Lean blowout limits of radial-vane mixer. Afterburner-inlet temperature, 1660° R; afterburner length, $4\frac{1}{2}$ feet.

[redacted]

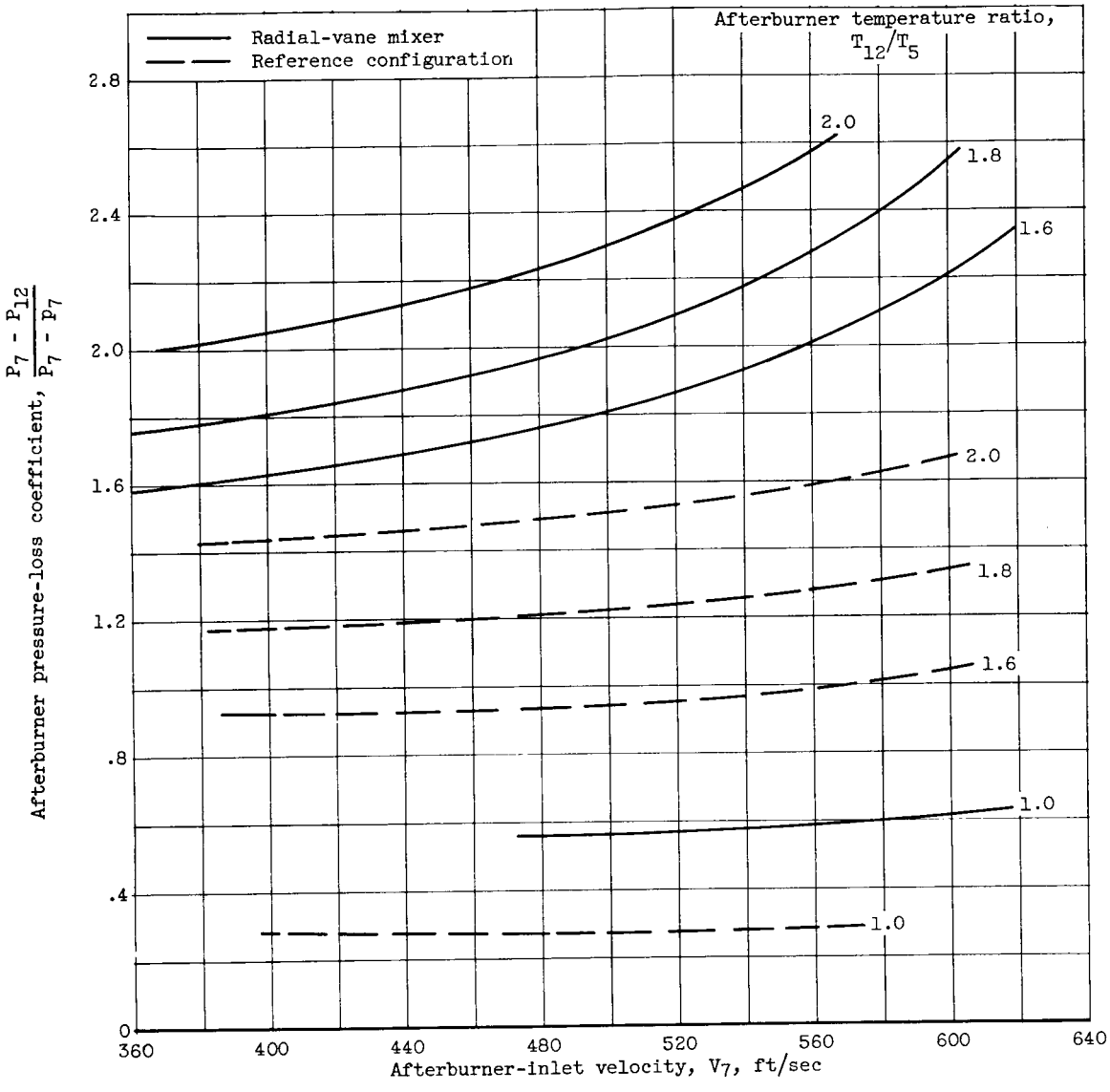

Figure 25. - Afterburner pressure-loss coefficient of radial-vane mixer. Afterburner-inlet temperature, 1660° R; afterburner-inlet pressures, 750 to 1270 pounds per square foot absolute; afterburner length, $4\frac{1}{2}$ feet.

[redacted]